Time dependent changes in feeding behavior and energy balance associated with weight gain in mice fed obesogenic diets

Payam A. Fathi[1], Michelle B. Bales[1,†], Julio E. Ayala[1,2,3*]

[1]Department of Molecular Physiology & Biophysics, Vanderbilt University School of Medicine, Nashville, TN, 37232

[2]Vanderbilt Mouse Metabolic Phenotyping Center, Nashville, TN, 37232

[3]Vanderbilt Center for Addiction Research, Nashville, TN, 37223

[†]Current address: Department of Psychology, Florida State University, Tallahassee, FL, 32306

*Corresponding author:

2201 Garland Avenue

702 Light Hall

Nashville, TN, 37232

Email: julio.e.ayala@vanderbilt.edu

Phone: (615) 323-7252

Disclosure: The authors declare no conflict of interest

What is already known about this subject?

- Obesity is associated with dysregulated homeostatic mechanisms.
- Increased caloric consumption contributes to obesity.
- Obese rodents tend to eat larger, more frequent meals.

What are the new findings in your manuscript?

- Exposure to obesogenic diets promotes transient attempts to maintain weight homeostasis.
- After ~2 weeks, caloric hyperphagia exceeds increased energy expenditure, promoting weight gain.
- This is associated with consumption of larger, more frequent meals.

How might your results change the direction of research or the focus of clinical practice?

Our findings suggest that molecular studies focusing on mechanisms that regulate meal size and frequency, particularly those engaged during the first ~2 weeks of obesogenic diet feeding that eventually fail, can provide unique insight into the etiology of obesity.

Abstract

Obesity is characterized by dysregulated homeostatic mechanisms resulting in positive energy balance, yet when this dysregulation occurs is unknown. We assessed the time course of alterations to behaviors promoting weight gain in male and female mice switched to obesogenic 60% or 45% high fat diet (HFD). Switching mice to obesogenic diets promotes transient bouts of hyperphagia during the first 2 weeks followed by persistent caloric hyperphagia. Energy expenditure increases but not sufficiently to offset increased caloric intake, resulting in a sustained net positive energy balance. Hyperphagia is associated with consumption of calorically larger meals (impaired satiation) more frequently (impaired satiety) particularly during the light-cycle. Running wheel exercise delays weight gain in 60% HFD-fed male mice by enhancing satiation and increasing energy expenditure. However, exercise effects on satiation are no longer apparent after 2 weeks, coinciding with weight gain. Thus, exposure to obesogenic diets engages homeostatic regulatory mechanisms for ~2 weeks that ultimately fail, and consequent weight gain is characterized by impaired satiation and satiety. Insights into the etiology of obesity can be obtained by investigating changes to satiation and satiety mechanisms during the initial ~2 weeks of HFD exposure.

Introduction

Obesity results from caloric intake exceeding energy expenditure (EE). A general model for body weight regulation posits that weight gain triggers feedback mechanisms primarily in the central nervous system to subsequently decrease caloric intake, increase EE, and consequently reduce body weight (1). Obesity has been characterized as being associated with defects in these feedback mechanisms. However, evidence that these mechanisms are dysregulated has primarily been obtained comparing lean and obese subjects (mice, rats, humans). This is potentially problematic because homeostatic mechanisms may be preserved in obesity to defend elevated body weight (2, 3). Therefore, characterizing changes in parameters that regulate body weight prior to obesity onset can provide insights into potential mechanisms associated with excess weight gain.

Studies in rats show exposure to a high-fat diet (HFD) promotes a large, yet transient increase in caloric intake followed by sustained, slightly elevated daily caloric intake characterized by increased meal size and meal rate by calories but decreased meal number (4–7). These phenotypes are relevant since rats prone to greater weight gain consume more calories on a per meal basis without altering meal numbers (4, 7). Mice show a similar pattern characterized by a transient increase in caloric intake when switched to a HFD followed by a progressive decrease in calories consumed (8–11). A limitation of these studies is that HFD exposure was brief (3-7 days), and the primary endpoint for consumption was gross food intake. More nuanced factors that could influence weight gain, such as meal patterns, were not assessed. The importance of

this limitation is highlighted by the fact that genetic mouse models of obesity display increased meal size without increased daily caloric intake (12–15).

Sex and timing of exposure to obesogenic diets also affect weight gain. Male rodents increase caloric intake and body weight more than female rodents (16, 17). Mice fed obesogenic diets only during the light phase gain more weight than mice fed the same diet only during the dark phase (18). Access to HFD rapidly disrupts circadian food intake patterns, and mice no longer consume the majority of meals during the dark cycle (19).

Taken together, factors such as meal patterns, sex, and timing of food intake influence weight gain associated with obesogenic diets. When these factors are altered during the progression towards obesity is unknown. The present studies investigated the time scale and magnitude of changes to these components during the progression towards obesity. Our findings demonstrate that upon exposure to HFD, behaviors and metabolic phenotypes engaged to prevent weight gain rapidly become dysregulated. Furthermore, the magnitude of these changes is influenced by the type of obesogenic diet, sex, and light vs. dark cycles. This provides a blueprint for investigating molecular mechanisms whose dysregulation contributes to developing obesity.

Methods

91 ***Animals***

92 Male and female C57Bl6/J mice were studied at 10-12 weeks of age. In-house breeders were fed
93 "breeder" diet (5LJ5 – PicoLab Mouse Diet, LabDiet) and offspring were placed on chow (5L0D
94 – PicoLab Rodent Diet) at weaning (21 days). Experiments were conducted within an 18-month
95 period in offspring produced by multiple simultaneous breeders from the same founders to
96 minimize genetic drift. Mice were maintained on a 12-12 light-dark cycle (0600-1800) at 23°C.
97 Experimental procedures were approved by the Institutional Animal Care and Use Committee
98 at Vanderbilt University.

99 ***Diet Switch and Running Wheel Experiments***

100 Mice were single housed in Promethion Metabolic chambers (Sable Systems International) with
101 ad-lib access to chow (2.86 kCal/gram; PicoLab Rodent Diet 5L0D) for 5-7 days. Mice were then
102 switched to 60% HFD (5.24 kCal/gram; Research Diets Inc, D12492) for 4 weeks or 45% HFD
103 (4.73 kCal/gram; Research Diets Inc. D12451) for 3 weeks. A separate cohort was switched to
104 60% HFD or remained on chow for 3 weeks. For wheel running experiments, single-housed
105 male mice had access to chow and locked running wheels for 5 days. Mice were then switched
106 to 60% HFD and were randomly selected to remain with running wheels locked or have
107 running wheels unlocked for 4 weeks. External interventions (e.g., adding food/water, changing
108 cages) are indicated in each figure.

109 ***Metabolic Measurements***

110 Food intake, water intake, locomotor activity, respiratory exchange ratio, and EE were
111 continuously measured across five-minute intervals. Energy balance was determined by
112 subtracting total EE from energy intake across 12h light-dark cycles. Total EE for each light-dark
113 cycle was calculated as the average EE over the 12h time interval multiplied by 12. Energy
114 intake was calculated by multiplying the mass of food consumed over the corresponding 12h-
115 intervals with the diet caloric density. A technical failure eliminated locomotor activity data
116 after week 1 in 60% HFD-fed females. Body weights were measured weekly and body
117 composition before and after the HFD period was obtained by NMR (Bruker Optics).

118 ***Meal Parameters***

119 A meal was defined as food removal spanning at least 30 seconds, a minimum of 10 milligrams
120 to account for inherent sensor limitations, a maximum of 500 milligrams to account for spillage,
121 and a threshold of 5 minutes for inter-meal intervals based on prior rodent literature (20–23).
122 60% HFD was packed in the hopper to reduce spillage. Cages were inspected daily for excessive
123 spillage (food on cage bottom) and noted. If total food intake and meal number for a given day
124 was greater than 1.5x standard deviation of the mean for its respective feeding period, then this
125 was considered excessive spillage, and intake and meal pattern data for that day were excluded.
126 Excessive spillage was only observed with the 45% HFD experiments.

127 ***Meal Type Analysis***

128 Quartile distributions for meal types were defined by assembling meal sizes from all chow-fed
129 male mice to determine the following meal types: Type I: 10 – <60 mg; Type II: 60 – <160 mg;
130 Type III: 160 – <280 mg; and Type IV: >280 mg. Meal types were compared by determining the

weekly proportion of a given meal type within each animal across each week. Parts of whole analysis used compiled averages of meal types across sex and diet groups. Histograms were generated using bin sizes of 20 mg or .2 kCal and curve-fit using non-linear regression.

Statistical Analysis

Raw data were processed using the Sable Systems Macro Interpreter (v23.6). Graphs were generated and data statistically analyzed using repeated measures one-way ANOVA and Tukey's post-hoc or two-way ANOVA with the Sidak's post-hoc as necessary using GraphPad Prism (v10). Significance was set at $p<0.05$. Figures were assembled using Adobe Illustrator (v28.0).

Results

Metabolic phenotypes in mice switched to 60% HFD

When switching male mice to 60% HFD, food intake by mass is higher at week 4 of 60% HFD (**Figure 1A**), with a tendency for higher light cycle mass consumption throughout the HFD period (**Supplemental Figure 1A-B**). Food intake by mass is unaffected in female mice switched to 60% HFD (**Figure 1D**) during both cycles (**Supplemental Figure 1C-D**). Accounting for caloric density, both sexes display two cycles of rapid increases and decreases in calories consumed during the first 2 weeks of 60% HFD exposure followed by a sustained elevation in daily caloric intake (**Figure 1B, 1E**). This occurs during both light and dark cycles

150 (**Supplemental Figure 1E-H**). This pattern does not correspond with interventions such as
151 restocking of food or cage changes.

152 Switching to 60% HFD increases EE in males and females (**Figure 1C, 1F**) during both light and
153 dark cycles (**Supplemental Figure 1I-L**). Accounting for changing body weight, analysis of
154 covariance (ANCOVA) shows EE remains higher during the HFD period in males and trends
155 higher in females (**Supplemental Figure 2A**). Daily EE follows a similar pattern as caloric
156 intake, characterized by transient increases upon switching to the HFD followed by a sustained
157 increase after 2 weeks of the diet switch (**Figure 1C, 1F**). Male and female mice display
158 sustained positive energy balance and increasing body weight starting on week 2 of HFD
159 exposure (**Figure 1G-L**). Lean and fat mass increase in 60% HFD-fed male mice and tend to
160 increase in female mice (**Supplemental Figure 2B**).

161 Respiratory exchange ratio (RER) decreases upon exposure to 60% HFD in both sexes
162 (**Supplemental Figure 2C-D**), most robustly during the dark cycle (**Supplemental Figure 1M-**
163 **P**). Switching to 60% HFD rapidly decreases water intake and locomotor activity in both sexes
164 (**Supplemental Figure 2E-H**) primarily due to changes during the dark cycle (**Supplemental**
165 **Figure 1Q-W**).

166 ***Meal patterns in mice switched to 60% HFD***

167 Meal numbers rapidly increase in both sexes and are sustained throughout the 60% HFD period
168 (**Figure 2A-B**) in both light and dark cycles (**Supplemental Figure 3A-D**). Inter-meal interval
169 and meal duration decreases in both sexes (**Figure 2C-F**), with robust effects on inter-meal
170 interval during the light cycle (**Supplemental Figure 3E-H**) and meal duration during both

171 cycles (**Supplemental Figure 3I-L**). Meal size by mass decreases in male and female mice
172 (**Figure 2G-H**) primarily during the dark cycle (**Supplemental Figure 3M-P**). Accounting for
173 caloric density, meal size significantly increases in male mice after the second week of 60% HFD
174 exposure but only trends higher in female mice (**Figure 2I-J**). Male mice primarily increase meal
175 caloric content during the light cycle (**Supplemental Figure 3Q-R**), and female mice do so
176 during the dark cycle (**Supplemental Figure 3S-T**). There are transient increases and attempts
177 to restore meal size during the first two weeks of 60% HFD exposure. Rates of meal
178 consumption by mass or caloric content increase upon switching to 60% HFD in both males and
179 females (**Figure 2K-N**) primarily during the light cycle (**Supplemental Figure 3U-AB**).

180 Changes to metabolic and meal parameters in male mice switched to 60% HFD are not observed
181 in mice remaining on chow for 3 weeks (**Supplemental Figure 4**). Furthermore, male mice gain
182 more weight even though they increase EE more robustly than female mice (**Supplemental**
183 **Figure 5C-D**). Male mice display a greater increase in meal rates than females (**Supplemental**
184 **Figure 5I-J**).

185 ***Metabolic phenotypes in mice switched to 45% HFD***

186 When switched to 45% HFD, food intake by mass transiently increases in both sexes (**Figure 3A,**
187 **3D**) during light and dark cycles (**Supplemental Figure 6A-D**). Caloric intake increases during
188 weeks 1 and 3 (**Figure 3B, 3E**), and there is a tendency for this to occur during both light and
189 dark cycles (**Supplemental Figure 6E-H**). Both sexes rapidly increase EE (**Figure 3C, 3F**) during
190 the light and dark cycles (**Supplemental Figure 6I-L**). ANCOVA accounting for body weight
191 changes shows EE significantly increases in male mice and trends higher in female mice

192 (**Supplemental Figure 7A**). Energy balance becomes more positive and body weights gradually
193 increase in both sexes after switching to 45% HFD (**Figure 3G-L**). Lean and fat mass increase in
194 45% HFD-fed male mice but only lean mass increases in female mice (**Supplemental Figure 7B**).

195 Switching to 45% HFD decreases RER and water intake in both males and females, and there is
196 only a significant activity decrease in males (**Supplemental Figure 7C-M**). These decreases are
197 observed almost exclusively during the dark cycle (**Supplemental Figure 6M-X**).

198 ***Meal patterns in mice switched to 45% HFD***

199 Mice switched to 45% HFD display no significant change in meal number or inter-meal interval
200 in either sex (**Figure 4A-D**) during both light and dark cycles (**Supplemental Figure 8A-D**).
201 Meal duration significantly decreases in both sexes (**Figure 4E-F**) during light and dark cycles
202 (**Supplemental Figure 8I-L**). Meal size by mass is unaffected in male mice and tends to decrease
203 in female mice (**Figure 4G-H**) primarily due to effects during the light cycle (**Supplemental**
204 **Figure 8M-P**). Accounting for caloric density, caloric intake per meal increases in male mice,
205 primarily during the dark cycle, but remains unaltered in female mice (**Figure 4I-J**,
206 **Supplemental Figure 8Q-T**). Meal rates by mass and caloric content increase in both sexes and
207 during both light and dark cycles (**Figure 4M-N, Supplemental Figure 8U-AB**). Mice switched
208 to 45% HFD display significant food spillage, so intake and meal patterns likely overestimate
209 actual intake and contribute to increased data variability.

210 Females gain less weight than males when switched to 45% HFD, and this is associated with a
211 greater increase in EE in females (**Supplemental Figure 9C-D**). Males display greater increases
212 in meal rates, significantly so at 2 weeks of 45% HFD exposure (**Supplemental Figure 9I-J**).

Meal-typing in mice switched to HFD

Meals of very low mass and caloric content comprise the largest set of meals consumed during the chow period (**Figure 5A-D**). When switched to 60% HFD, male mice decrease consumption of meals of very low and larger masses (**Figure 5A**), resulting in a rightward shift towards a larger proportion of meals with higher caloric content (**Figure 5B**). Female mice switched to 60% HFD decrease the proportion of large meals and increase the proportion of small meals consumed (**Figure 5C**), but the proportion of meals with higher caloric content increases (**Figure 5D**). When switched to 45% HFD, there is a leftward shift in meal mass histograms in both male and female mice with a corresponding flattening of histogram spread in meal size by calories (**Figure 5E-H**).

Using quartile distribution of meal sizes by mass in chow-fed male mice to yield four meal types (**Figure 5I** and **Methods**), male mice switched to 60% HFD increase the proportion of type II meals consumed while decreasing the proportion of very small type I meals and displaying a trend towards decreasing the proportion of large and very large type III and type IV meals (**Figure 5J, 5N**). This is observed across light and dark cycles (**Supplemental Figure 10A-D**). Female mice switched to 60% HFD increase the proportion of type II meals and decrease the proportion of very large type IV meals consumed, but they also increase the proportion of very small type I meals consumed (**Figure 5K, 5O**). These shifts are primarily observed during the dark cycle (**Supplemental Figure 10A-D**). Similar shifts are observed in mice switched to 45% HFD (**Figure 5L, 5M, 5P, 5Q** and **Supplemental Figure 10E-H**).

233 ***Metabolic phenotypes and meal patterns in mice switched to 60% HFD with running wheel***
234 ***access***

235 We investigated whether running wheel activity increases EE sufficiently to offset the caloric
236 content of consuming 60% HFD. Food intake is similar in mice with active running wheels
237 (Wheels Unlocked) and mice with inactive running wheels (Wheels Locked), with similar
238 patterns of transient changes during the first ~2 weeks culminating in a sustained increase in
239 daily caloric intake (**Figure 6A-B**). EE is higher in the Wheels Unlocked group (**Figure 6C**,
240 **Supplemental Figure 11A** for ANCOVA) due to effects during the dark cycle (**Supplemental**
241 **Figure 11B**). This reduces the deviation towards positive energy balance in the Wheels
242 Unlocked group, although net energy balance is not significantly different between groups
243 (**Figure 6D-E, Supplemental Figure 11C**). The Wheels Unlocked group is protected against
244 significant body weight gain during the first two weeks of 60% HFD (**Figure 6F, Supplemental**
245 **Figure 11D**). However, mice with access to active running wheels begin to gain weight after the
246 second week, and this is associated with increased food and energy intake during the dark cycle
247 (**Supplemental Figure 12A-B**).

248 The Wheels Unlocked group displays a greater increase in meal number compared to the
249 Wheels Locked group during the first week (**Figure 6G**), mainly during the dark cycle
250 (**Supplemental Figure 12C**). Inter-meal interval and meal duration decrease equally in both
251 groups (**Figure 6H-I, Supplemental Figure 12D-E**). Access to active running wheels lowers
252 meal size by mass and calories on the first week of 60% HFD during both the light and dark
253 cycles (**Figure 6J-K; Supplemental Figure 12F-G**). This is no longer evident after week 2,

254 coincident with greater deviations towards positive energy balance and weight gain in mice
255 with access to active running wheels. Meal rates are not significantly different between groups
256 (**Figure 6L-M, Supplemental Figure 12H-I**). The proportion of meals consumed with a lower
257 caloric content is higher in the Wheels Locked group (**Figure 6N-O**). Furthermore, both groups
258 increase their consumption of type II meals and decrease their consumption of very large type
259 IV meals, but mice with access to active running wheels also increase the consumption of very
260 small type I meals and have a larger decrease in the proportion of very large type IV meals
261 consumed during the first week of 60% HFD exposure (**Supplemental Figure 12J-L**).

262 RER is significantly lower in mice with running wheel access during the first two weeks
263 following diet switch (**Supplemental Figure 11E-F**). Water intake decreases equally in both
264 groups following 60% HFD exposure, although dark cycle water intake tends to be higher in the
265 Wheels Unlocked group (**Supplemental Figure 11G-H**). Off-wheel activity decreases in both
266 groups when switched to 60% HFD, although mice with active running wheels have higher off-
267 wheel activity during the last two weeks of diet exposure, particularly during the dark cycle
268 (**Supplemental Figure 11I-J**). Wheel running activity progressively increases and levels out by
269 week four and is highest during the dark cycle (**Supplemental Figure 11K-L**).

270

271

272

273

Discussion

Our results reveal the time course over which mice engage processes to maintain neutral energy balance and when these processes ultimately fail in the presence of HFD. Obtaining these results in the genetically tractable mouse can be leveraged towards investigating mechanisms characterizing the transition from maintaining weight homeostasis to the failure of these attempts. Furthermore, we provide analyses of other parameters, such as meal size, that we hypothesize are significant contributors to the propensity to gain weight.

Short-term (3-7 day) exposure to HFD promotes transient hyperphagia in mice (8–11). We show that transient hyperphagia followed by attempts to restore normal energy intake occurs during the first ~14 days of HFD exposure, and mice then display sustained hyperphagia. This suggests that homeostatic mechanisms are engaged during the first ~2 weeks of HFD exposure, but they ultimately fail or are overtaken by other factors such as hedonic mechanisms. Identifying mechanisms engaged during the first 2 weeks of HFD exposure that then fail or are overcome will provide important information about molecular targets essential for weight control. Feeding during early stages of HFD exposure is regulated by astrocyte-mediated control of brainstem glutamatergic neurotransmission from vagal inputs (11). Furthermore, the anorectic effect of cholecystokinin (CCK), a hormone regulating meal size via vagal inputs from the gut (24), is impaired in male mice after 5 weeks on HFD (17). Collectively, these findings suggest that vagal mechanisms linking the gut and brainstem are targets for future studies investigating processes contributing to weight gain in response to HFD.

294 Our findings agree with studies in rats showing increased meal size by caloric content upon
295 HFD exposure (4–7). Meal size by caloric content is a strong predictor of weight gain in rats (4,
296 7). An increase in meal size is indicative of impaired satiation – fullness during meal ingestion.
297 CCK-induced satiation is impaired in male mice after 5 weeks on HFD (17). Obesogenic diets
298 also impact satiation by impairing vagal afferent responsiveness to distension and changes in
299 gastric emptying (25, 26). Since these studies on CCK and vagal responsiveness were conducted
300 in response to long-term HFD exposure, it is unclear whether these factors are a cause or
301 consequence of weight gain. Our findings that meal size increases prior to weight gain strongly
302 suggest that impaired satiation contributes to obesity. Contrasting results in rats (4, 5), we show
303 meal number increases in mice exposed to HFD, suggesting that satiety – fullness between
304 meals – is also impaired and highlights the need to study mechanisms that integrate satiation
305 and satiety as contributors to weight gain.

306 There are interesting sex differences in the response to HFD. Male mice increase the proportion
307 of slightly larger (type II) meals at the expense of smaller (type I) meals typically consumed
308 during the chow period. Females also increase the proportion of type II meals consumed but
309 partially offset this by increasing the proportion of type I meals. Male mice also display greater
310 increases in meal rates relative to female mice. This likely contributes to the more pronounced
311 weight gain that is typically observed in male vs. female mice. In support of this, increased
312 energy intake and meal sizes are observed in male relative to female mice following 5 weeks on
313 HFD (17). These sex differences can be leveraged to investigate potential mechanisms regulating
314 meal patterns such as steroid hormone signaling (27–29).

315 Our observation that exposure to HFD increases energy intake during the light cycle highlights
316 the relative importance of meal timing noted in humans and rodents. Increased light cycle
317 energy intake is associated with greater weight gain in rodents (18, 30), and caloric consumption
318 later in the day is associated with greater weight gain in humans (31–34). The present studies
319 demonstrate increased caloric intake during the light cycle associated with more frequent and
320 rapid intake of larger meals in HFD-fed mice, particularly male mice. HFD impairs vagal
321 afferent circadian rhythms (35, 36), which may contribute to increased daytime meal size.
322 Increasing intestinal glucagon-like peptide-1 (GLP-1) decreases daytime food intake in mice in a
323 vagal GLP-1 receptor-mediated manner, presumably through modulating meal termination (37,
324 38). Thus, future studies should address whether defects in these mechanisms occur in a time
325 scale corresponding to the changes in feeding behavior we demonstrate in the present studies.

326 Male and female mice experience quantitatively similar increases in absolute EE when switched
327 to HFD, but this is not sufficient to compensate for the increased caloric intake. Protection from
328 weight gain in female relative to male mice may be driven by the ability of female mice to better
329 utilize fat (9, 17), supported by our data showing lower relative RER in female compared to
330 male mice switched to a 60% HFD. This also agrees with recent studies showing that female
331 mice balance energy expenditure and intake more efficiently than do male mice (39)

332 EE increases in response to HFD even as locomotor activity decreases, as previously observed
333 (10, 40). Decreased locomotor activity in HFD-fed mice accounts for >60% of weight gain (40).
334 Providing male mice with access to running wheels when switched to 60% HFD significantly
335 increases EE and partially mitigates the shortfall between EE and caloric intake, thus reducing

336 weight gain, as previously shown (41). Satiation is also enhanced in mice with wheel running
337 access, and we speculate this further contributes to reduced weight gain. However, after ~2
338 weeks of HFD/running wheel exposure, enhanced satiation is no longer apparent and mice with
339 wheel running access begin to gain weight. These findings further emphasize the potential role
340 of meal size as a contributor to weight gain in the presence of obesogenic diets.

341 In sum, our study provides insights into how time-dependent changes in feeding behaviors
342 following obesogenic diet exposure can modify weight gain. Although previous studies in rats
343 show similar findings, the present studies conducted in the more genetically tractable mouse
344 provide the foundation for future studies to investigate molecular mechanisms relevant to the
345 regulation of meal patterns and weight gain. Furthermore, our analyses using different HFD
346 and comparing sexes not only further emphasize the importance of the association between
347 meal patterns and weight gain but also highlight phenotypes that can be used in future studies
348 on the contribution of diet composition and sex on weight gain.

349 ***Considerations***

350 Our studies were conducted at a standard housing temperature for most animal facilities (23°C),
351 which is below the thermoneutral temperature for mice (~28-30°C). Temperature impacts EE
352 and weight gain in a sex-dependent manner in mice (39), so repeating these experiments at a
353 higher temperature will likely yield different outcomes regarding EE and meal patterns. The
354 present studies did not use matched low-fat diets for each HFD. The magnitude of metabolic
355 changes may be different when using matched low-fat diets. Although we established visual
356 and threshold parameters for food spillage (see **Methods**), there is inherent inaccuracy in food

intake measurements resulting from food spillage and caching occurring with any metabolic chamber. We did not measure fecal energy content, so the energy balance calculation assumes complete energy absorption. Finally, interpreting running wheel results must consider the fact that mice were provided with two rewarding stimuli simultaneously (HFD and running). Our colleague Dr. Nathan Winn shows that switching mice to a 60% HFD after 5 weeks of running wheel access further increases running wheel activity, but increased caloric intake is equivalent to mice switched to 60% HFD without prior access to running wheels (personal communication).

Author Contributions

Conceptualization: JEA, MBB, PF; Methodology: JEA, MBB, PF; Analysis: JEA, PF; Writing: JEA, PF; Funding: JEA. All authors reviewed and have approved the final version of this manuscript.

Acknowledgements and Funding

We would like to thank Dr. Louise Lantier and Merrygay James for their assistance. Promethion metabolic chamber studies were conducted within the Vanderbilt Mouse Metabolic Phenotyping Center (VMMPC) which is supported by NIH grant U2C0595637, shared instrument grant S10OD028455 (JEA). This work was funded by NIH grants F31-DK127728 (PF), T32-DK07563 (PF, MBB), and R01-DK132852 (JEA).

377 **References**

378 1. Myers MG, Affinati AH, Richardson N, Schwartz MW. Central nervous system
379 regulation of organismal energy and glucose homeostasis. *Nat Metab* 2021;3:737–750.

380 2. Lund C, Ranea-Robles P, Falk S, *et al.* Protection against overfeeding-induced weight
381 gain is preserved in obesity but does not require FGF21 or MC4R. *Nat Commun* 2024;15:1192.

382 3. Schwartz MW, Seeley RJ, Zeltser LM, *et al.* Obesity Pathogenesis: An Endocrine Society
383 Scientific Statement. *Endocr Rev* 2017;38:267–296.

384 4. Furnes MW, Zhao C-M, Chen D. Development of obesity is associated with increased
385 calories per meal rather than per day. A study of high-fat diet-induced obesity in young rats.
386 *Obes Surg* 2009;19:1430–8.

387 5. Treesukosol Y, Moran TH. Analyses of meal patterns across dietary shifts. *Appetite*
388 2014;75:21–9.

389 6. Melhorn SJ, Krause EG, Scott KA, *et al.* Acute exposure to a high-fat diet alters meal
390 patterns and body composition. *Physiol Behav* 2010;99:33–9.

391 7. Farley C, Cook JA, Spar BD, Austin TM, Kowalski TJ. Meal pattern analysis of diet-
392 induced obesity in susceptible and resistant rats. *Obes Res* 2003;11:845–851.

393 8. Enriquez JR, McCauley HA, Zhang KX, *et al.* A dietary change to a high-fat diet initiates
394 a rapid adaptation of the intestine. *Cell Rep* 2022;41:111641.

395 9. Oraha J, Enriquez RF, Herzog H, Lee NJ. Sex-specific changes in metabolism during the
396 transition from chow to high-fat diet feeding are abolished in response to dieting in C57BL/6J
397 mice. *Int J Obes (Lond)* 2022;46:1749–1758.

398 10. Kless C, Rink N, Rozman J, Klingenspor M. Proximate causes for diet-induced obesity in
399 laboratory mice: a case study. *Eur J Clin Nutr* 2017;71:306–317.

400 11. Clyburn C, Carson KE, Smith CR, Travagli RA, Browning KN. Brainstem astrocytes
401 control homeostatic regulation of caloric intake. *J Physiol* 2023;601:801–829.

402 12. Strohmayer AJ, Smith GP. The meal pattern of genetically obese (ob/ob) mice. *Appetite*
403 1987;8:111–23.

404 13. Ladenheim EE, Hampton LL, Whitney AC, White WO, Battey JF, Moran TH. Disruptions
405 in feeding and body weight control in gastrin-releasing peptide receptor deficient mice. *J*
406 *Endocrinol* 2002;174:273–81.

407 14. Lin L, Nuotio-Antar AM, Ma X, Liu F, Fiorotto ML, Sun Y. Ghrelin receptor regulates
408 appetite and satiety during aging in mice by regulating meal frequency and portion size but not
409 total food intake. *J Nutr* 2014;144:1349–55.

410 15. Richard CD, Tolle V, Low MJ. Meal pattern analysis in neural-specific
411 proopiomelanocortin-deficient mice. *Eur J Pharmacol* 2011;660:131–8.

412 16. Yang Y, Smith DL, Keating KD, Allison DB, Nagy TR. Variations in body weight, food
413 intake and body composition after long-term high-fat diet feeding in C57BL/6J mice. *Obesity*
414 2014;22:2147–2155.

415 17. Huang K-P, Ronveaux CC, Knotts TA, Rutkowsky JR, Ramsey JJ, Raybould HE. Sex
416 differences in response to short-term high fat diet in mice. *Physiol Behav* 2020;221:112894.

417 18. Arble DM, Bass J, Laposky AD, Vitaterna MH, Turek FW. Circadian timing of food
418 intake contributes to weight gain. *Obesity (Silver Spring)* 2009;17:2100–2.

419 19. Espinosa-Carrasco J, Burokas A, Fructuoso M, *et al.* Time-course and dynamics of
420 obesity-related behavioral changes induced by energy-dense foods in mice. *Addiction Biology*
421 2018;23:531–543.

422 20. Zorrilla EP, Inoue K, Fekete EM, Tabarin A, Valdez GR, Koob GF. Measuring meals:
423 structure of prandial food and water intake of rats. *Am J Physiol Regul Integr Comp Physiol*
424 2005;288:R1450-67.

425 21. Rathod YD, Di Fulvio M. The feeding microstructure of male and female mice. *PLoS One*
426 2021;16:e0246569.

427 22. Stengel A, Goebel M, Wang L, *et al.* Activation of brain somatostatin 2 receptors
428 stimulates feeding in mice: analysis of food intake microstructure. *Physiol Behav* 2010;101:614–
429 22.

430 23. Gannon KS, Smith JC, Henderson R, Hendrick P. A system for studying the
431 microstructure of ingestive behavior in mice. *Physiol Behav* 1992;51:515–21.

432 24. Raybould HE. Mechanisms of CCK signaling from gut to brain. *Curr Opin Pharmacol*
433 2007;7:570–4.

434 25. Loper H, Leinen M, Bassoff L, *et al.* Both high fat and high carbohydrate diets impair
435 vagus nerve signaling of satiety. *Sci Rep* 2021;11:10394.

436 26. Kentish SJ, Frisby CL, Kritas S, *et al.* TRPV1 Channels and Gastric Vagal Afferent
437 Signalling in Lean and High Fat Diet Induced Obese Mice. *PLoS One* 2015;10:e0135892.

438 27. Petersen S. The temporal pattern of feeding over the oestrous cycle of the mouse. *Anim*
439 *Behav* 1976;24:939–955.

440 28. Alonso-Caraballo Y, Ferrario CR. Effects of the estrous cycle and ovarian hormones on
441 cue-triggered motivation and intrinsic excitability of medium spiny neurons in the Nucleus
442 Accumbens core of female rats. *Horm Behav* 2019;116:104583.

443 29. Lenert ME, Chaparro MM, Burton MD. Homeostatic Regulation of Estrus Cycle of
444 Young Female Mice on Western Diet. *J Endocr Soc* 2021;5.

445 30. Olsen MK, Choi MH, Kulseng B, Zhao C-M, Chen D. Time-restricted feeding on
446 weekdays restricts weight gain: A study using rat models of high-fat diet-induced obesity.
447 *Physiol Behav* 2017;173:298–304.

448 31. Zhao D, Guallar E, Woolf TB, *et al.* Association of Eating and Sleeping Intervals With
449 Weight Change Over Time: The Daily24 Cohort. *J Am Heart Assoc* 2023;12:e026484.

450 32. Ruddick-Collins LC, Morgan PJ, Fyfe CL, *et al.* Timing of daily calorie loading affects
451 appetite and hunger responses without changes in energy metabolism in healthy subjects with
452 obesity. *Cell Metab* 2022;34:1472-1485.e6.

453 33. Jakubowicz D, Barnea M, Wainstein J, Froy O. High caloric intake at breakfast vs. dinner
454 differentially influences weight loss of overweight and obese women. *Obesity (Silver Spring)*
455 2013;21:2504–12.

456 34. Bo S, Musso G, Beccuti G, *et al.* Consuming more of daily caloric intake at dinner
457 predisposes to obesity. A 6-year population-based prospective cohort study. *PLoS One*
458 2014;9:e108467.

459 35. Kentish SJ, Hatzinikolas G, Li H, Frisby CL, Wittert GA, Page AJ. Time-Restricted
460 Feeding Prevents Ablation of Diurnal Rhythms in Gastric Vagal Afferent Mechanosensitivity
461 Observed in High-Fat Diet-Induced Obese Mice. *J Neurosci* 2018;38:5088–5095.

462 36. Kentish SJ, Vincent AD, Kennaway DJ, Wittert GA, Page AJ. High-Fat Diet-Induced
463 Obesity Ablates Gastric Vagal Afferent Circadian Rhythms. *J Neurosci* 2016;36:3199–207.

464 37. Borgmann D, Ciglieri E, Biglari N, *et al.* Gut-brain communication by distinct sensory
465 neurons differently controls feeding and glucose metabolism. *Cell Metab* 2021;33:1466-1482.e7.

466 38. Iwasaki Y, Sendo M, Dezaki K, *et al.* GLP-1 release and vagal afferent activation mediate
467 the beneficial metabolic and chronotherapeutic effects of D-allulose. *Nat Commun* 2018;9:113.

468 39. Morris EM, Noland RD, Allen JA, *et al.* Difference in Housing Temperature-Induced
469 Energy Expenditure Elicits Sex-Specific Diet-Induced Metabolic Adaptations in Mice. *Obesity*
470 *(Silver Spring)* 2020;28:1922–1931.

471 40. Bjursell M, Gerdin A-K, Lelliott CJ, *et al.* Acutely reduced locomotor activity is a major
472 contributor to Western diet-induced obesity in mice. *Am J Physiol Endocrinol Metab*
473 2008;294:E251-60.

474 41. Cho C, Ji M, Cho E, Yi S, Kim JG, Lee S. Chronic voluntary wheel running exercise
475 ameliorates metabolic dysfunction via PGC-1α expression independently of FNDC5/irisin
476 pathway in high fat diet-induced obese mice. *J Physiol Sci* 2023;73:6.

477

478

479

480

481

482 **Figure Legends**

483 **Figure 1. Food intake and energy balance in mice switched to 60% HFD.** Mice were placed in
484 metabolic chambers and were fed with chow for up to 6 days. Mice were then switched to 60%
485 HFD at day 0 (dashed line) and remained on 60% HFD for 28 days. (A-C, G, I, J) represent data
486 from male mice (black) and (D-F, H, K, L) represent data from female mice (pink). (A, D) Daily
487 and average weekly food intake by mass (grams). (B, E) Daily and average weekly caloric
488 intake. (C, F) Daily and average weekly energy expenditure. (G, H) Heat map showing shifts in
489 net daily energy balance. (I, K) Average weekly energy balance. (J, L) Average weekly body
490 weight. Arrows indicate external interventions such as adding food/water or cage changes. Data
491 are shown as mean ± SEM for *N*=8 per sex and were statistically analyzed using a repeated
492 measures one-way ANOVA with Tukey multiple comparison tests. P-value definitions: not-
493 significant (ns) >0.05, * <0.05, **<0.01, ***<0.001, **** <0.00001.

494

495 **Figure 2. Feeding behaviors in mice switched to 60% HFD.** Feeding behavior analysis in male
496 mice (black) and female mice (pink) switched from chow to 60% HFD in metabolic chambers at
497 day 0 (dashed line). (A) Daily and (B) average weekly meal numbers. (C) Daily and (D) average
498 weekly intermeal intervals. (E) Daily and (F) average weekly meal duration. (G) Daily and (H)
499 average weekly meal size by mass. (I) Daily and (J) average weekly meal size by calorie. (K)
500 Daily and (L) average weekly meal rate in grams consumed per minute. (M) Daily and (N)
501 average weekly meal rate in calories consumed per minute. Data are shown as mean ± SEM for
502 *N*=8 per sex and were statistically analyzed using a repeated measures one-way ANOVA with

503 Tukey multiple comparison tests. P-value definitions: not-significant (ns) >0.05, * <0.05, **<0.01,
504 ***<0.001, **** <0.00001.

505

506 **Figure 3. Food intake and energy balance in male and female mice switched to 45% HFD.**
507 Mice were placed in metabolic chambers and were fed with chow for 5 days. Mice were then
508 switched to 45% HFD at day 0 (dashed line) and remained on 45% HFD for 21 days. (A-C, G, I,
509 J) represent data from male mice (black) and (D-F, H, K, L) represent data from female mice
510 (pink). (A, D) Daily and average weekly food intake by mass (grams). (B, E) Daily and average
511 weekly caloric intake. (C, F) Daily and average weekly energy expenditure. (G, H) Heat map
512 showing shifts in net daily energy balance. Blank squares indicate days in which data were
513 excluded due to excessive spillage. (I, K) Average weekly energy balance. (J, L) Average weekly
514 body weight. Arrows indicate external interventions such as adding food/water or cage
515 changes. Data are shown as mean ± SEM for *N*=8 per sex and were statistically analyzed using a
516 repeated measures one-way ANOVA with Tukey multiple comparison tests. P-value definitions:
517 not-significant (ns) >0.05, * <0.05, **<0.01, ***<0.001, **** <0.00001.

518

519 **Figure 4. Feeding behaviors in mice switched to 45% HFD.** Feeding behavior analysis in male
520 mice (black) and female mice (pink) switched from chow to 45% HFD in metabolic chambers at
521 day 0 (dashed line). (A) Daily and (B) average weekly meal numbers. (C) Daily and (D) average
522 weekly intermeal intervals. (E) Daily and (F) average weekly meal duration. (G) Daily and (H)
523 average weekly meal size by mass. (I) Daily and (J) average weekly meal size by calorie. (K)

524 Daily and (L) average weekly meal rate in grams consumed per minute. (M) Daily and (N)
525 average weekly meal rate in calories consumed per minute. Data are shown as mean ± SEM for
526 *N*=8 per sex and were statistically analyzed using a repeated measures one-way ANOVA with
527 Tukey multiple comparison tests. P-value definitions: not-significant (ns) >0.05, * <0.05, **<0.01,
528 ***<0.001, **** <0.00001.

529

530 **Figure 5. Meal patterns of male and female mice fed obesogenic diets.** Meal size analysis in
531 male and female mice switched from chow to 60% HFD (A-D, J-K, N-O) for 4 weeks or 45%
532 HFD (E-H, L-M, P-Q) for 3 weeks. Histograms of meal size by (A) grams and (B) calories in
533 male and (C) grams and (D) calories in female mice switched to a 60% HFD. Histograms of meal
534 size by (E) grams and (F) calories in male and (G) grams and (H) calories in female mice
535 switched to a 45% HFD. Histogram bin sizes of 0.02 (range: 0-0.5) for meals by grams and bin
536 size of 0.2 (range: 0-3) for meals by calories. Non-linear regression was used to fit curves on each
537 graph. (I) Range of meal sizes in grams consumed by mice (n=16) during the chow feeding
538 period. Quartiles were used to determine cut-offs for meal types. Type 1: <60 mg, Type2: <160
539 mg, Type 3: <280 mg, and Type 4: >280 mg. Pie-charts depicting meal types across diet switch
540 week in (J) males and (K) females switched from chow to a 60% HFD and (L) males and (M)
541 females switched from chow to a 45% HFD. Percent frequency of meals by type across each
542 week of feeding in (N) males and (O) females switched from chow to a 60% HFD and (P) males
543 and (Q) females switched from chow to a 45% HFD. Data are shown as mean ± SEM for *N*=8 per
544 sex and were statistically analyzed using a repeated measures one-way ANOVA with Tukey

545 multiple comparison tests. P-value definitions: not-significant (ns) >0.05, * <0.05, **<0.01,
546 ***<0.001, **** <0.00001.

547

548 **Figure 6. Effects of running wheel access on feeding behavior and energy expenditure in**
549 **male mice switched to 60% HFD.** Male mice were placed in metabolic chambers with chow and
550 locked running wheels for 5 days. Mice were then switched to 60% HFD on day 0 (dashed line)
551 and concomitantly remained with locked wheels (wheels locked, black) or the running wheels
552 were unlocked (wheels unlocked, red) for 28 days. (A) Daily and average weekly food intake in
553 grams. (B) Daily and average weekly caloric intake. (C) Daily and average weekly energy
554 expenditure. (D) Heat map depicting net energy balance for each mouse across time after being
555 switched from normal chow to 60% HFD with locked or unlocked running wheels. (E) Average
556 net daily energy balance across each week of diet. (F) Average body weight across each week of
557 diet. Feeding behavior analysis depicting (G) daily and average weekly average meal number,
558 (H) daily and average weekly intermeal interval, (I) daily and average weekly meal duration, (J)
559 daily and average weekly meal size in grams, (K) daily and average weekly meal size in
560 calories, (L) daily and average weekly meal rates in grams per minute, and (M) daily and
561 average weekly meal rate in calories per minute. (N) Histograms of meal size by gram in bin
562 sizes of 0.02 (Range 0-0.5). (O) Histograms of meal size by calories in bin sizes of 0.2 (Range 0-3).
563 Non-linear regression was used to fit curves on each graph. Arrows indicate external
564 interventions such as adding food/water or cage changes. Data are shown as mean ± SEM for
565 *N*=8 per group and were statistically analyzed using a two-way ANOVA with Sidaks multiple

566 comparison tests. P-value definitions: not-significant (ns) >0.05, * <0.05, **<0.01, ***<0.001, ****
567 <0.00001.

568

569 **Supplemental Figure 1. Metabolic phenotyping of mice switched to 60% HFD separated by**
570 **light-dark cycle.** Metabolic phenotyping parameters in male and female mice switched from
571 chow to 60% HFD on day 0 (dashed lines) in metabolic chambers and divided by light (blue)
572 and dark (beige) cycles. (A) Daily food intake in grams in male and (C) female mice. Average
573 weekly food intake by mass in the light and dark cycle in (B) male mice and in (D) female mice.
574 (E) Daily caloric intake in male and (G) female mice. Average weekly caloric intake in the light
575 and dark cycle in (F) male mice and in (H) female mice. (I) Daily energy expenditure in male
576 and (K) female mice. Average weekly energy expenditure in the light and dark cycle in (J) male
577 mice and in (L) female mice. (M) Daily respiratory exchange ratio in male and (O) female mice.
578 Average weekly respiratory exchange ratio in the light and dark cycle in (N) male mice and in
579 (P) female mice. (Q) Daily water intake in male and (S) female mice. Average weekly water
580 intake in the light and dark cycle in (R) male mice and in (T) female mice. (U) Daily locomotor
581 activity in male and (W) female mice. Average weekly locomotor activity in the light and dark
582 cycle in (V) male mice and in (X) female mice. Locomotor activity data are only available for
583 first seven days of diet switch in female mice due to instrument malfunction for this feature.
584 Data are shown as mean ± SEM for *N*=8 per sex and were statistically analyzed using a repeated
585 measures one-way ANOVA with Tukey multiple comparison tests. P-value definitions: not-
586 significant (ns) >0.05, * <0.05, **<0.01, ***<0.001, **** <0.00001.

587

588 **Supplemental Figure 2. Metabolic phenotyping of mice switched to 60% HFD.** Metabolic
589 parameters in male (black) and female (pink) mice fed a chow diet and switched to 60% HFD
590 for 28 days. (A) ANCOVA of average weekly energy expenditure with body weight as a
591 covariate. (B) Body composition in chow-fed (Pre) and at the end of 28 days of HFD feeding
592 (Post). (C) Daily and average weekly respiratory exchange ratio in male and (D) female mice.
593 (E) Daily and average weekly water intake in male and (F) female mice. (G) Daily and average
594 weekly locomotor activity in male and (H) female mice. Locomotor activity data are only
595 available for first seven days of diet switch in female mice due to instrument malfunction for
596 this feature. Data are shown as mean ± SEM for *N*=8 per sex and were statistically analyzed
597 using a repeated measures one-way ANOVA with Tukey multiple comparison tests. P-value
598 definitions: not-significant (ns) >0.05, * <0.05, **<0.01, ***<0.001, **** <0.00001.

599

600 **Supplemental Figure 3. Feeding behaviors in mice switched to 60% HFD separated by light-**
601 **dark cycle.** Feeding behavior analysis in male and female mice switched from chow to 60%
602 HFD on day 0 (dashed lines) in metabolic chambers and divided by light (blue) and dark (beige)
603 cycles. (A) Daily and (B) average weekly meal number in male and (C) daily and (D) average
604 weekly meal number in female mice. (E) Daily and (F) average weekly inter-meal interval in
605 male mice and (G) daily and (H) average weekly inter-meal interval in female mice. (I) Daily
606 and (J) average weekly meal duration in male mice and (K) daily and (L) average weekly meal
607 duration in female mice. (M) Daily and (N) average weekly meal size by mass in male mice and

608 (O) daily and (P) average weekly meal size by mass in female mice. (Q) Daily and (R) average
609 weekly meal size by calorie in male mice and (S) daily and (T) average weekly meal size by
610 calorie in female mice. (U) Daily and (V) average weekly meal rate in grams per minute in male
611 mice and (W) daily and (X) average weekly meal rate in grams per minute in female mice. (Y)
612 Daily and (Z) average weekly meal rate in calories per minute in male mice and (AA) Daily and
613 (AB) average weekly meal rate in calories per minute in female mice. Data are shown as mean ±
614 SEM for *N*=8 per sex and were statistically analyzed using repeated measures one-way ANOVA
615 with Tukey multiple comparison tests. P-value definitions: not-significant (ns) >0.05, * <0.05,
616 **<0.01, ***<0.001, **** <0.00001.

617

618 **Supplemental Figure 4. Food intake, energy expenditure, and feeding behaviors in male mice**
619 **retained on chow or switched to 60% HFD.** Male mice were switched to 60% HFD on day 0 or
620 remained on chow for 21 days. (A) Daily food intake by mass and (B) average weekly food
621 intake by mass over 24h and during the light and dark cycle. (C) Daily energy intake by calorie
622 and (D) average weekly energy intake by calorie over 24h and during the light and dark cycle.
623 (E) Daily energy expenditure and (F) average weekly energy expenditure over 24h and during
624 the light and dark cycle. (G) Average weekly body weight. (H) Average weekly meal number by
625 24h, light cycle, and dark cycle in chow-fed mice. (I) Average meal size by mass by 24h, light
626 cycle, and dark cycle in chow-fed mice. (J) Average meal duration by 24h, light cycle, and dark
627 cycle in chow-fed mice. (K) Average inter-meal interval by 24h, light cycle, and dark cycle in
628 chow-fed mice. (L) Average weekly meal rate by mass by 24h, light cycle, and dark cycle in

629 chow-fed mice. Data are shown as mean ± SEM for *N*=4-12 per group and were statistically
630 analyzed using repeated measures one-way ANOVA with Tukey multiple comparison tests or
631 two-way ANOVA with Sidak multiple comparison test. P-value definitions: not-significant (ns)
632 >0.05, * <0.05, **<0.01, ***<0.001, **** <0.00001.

633

634 **Supplemental Figure 5. Effects of sex on 60% HFD-induced changes in metabolic parameters**
635 **and meal patterns.** Average weekly data are shown for male (black symbols) and female (pink
636 symbols) mice as both absolute values and values normalized to chow for each individual
637 mouse across 24-hour cycles. (A) Food intake by mass. (B) Energy intake by calorie. (C) Energy
638 expenditure. (D) Body weight. (E) Meal number. (F) meal size by mass. (G) Meal size by calorie.
639 (H) Meal duration. (I) Meal rate by mass. (J) Meal rate by calorie. Data are shown as mean ±
640 SEM for *N*=8 per sex and were statistically analyzed using two-way ANOVA with Sidak
641 multiple comparison test. P-value definitions: not-significant (ns) >0.05, * <0.05, **<0.01,
642 ***<0.001, **** <0.00001.

643

644 **Supplemental Figure 6. Metabolic phenotyping of mice switched to 45% HFD separated by**
645 **light-dark cycle.** Metabolic phenotyping parameters in male and female mice switched from
646 chow to 45% HFD on day 0 (dashed lines) in metabolic chambers and divided by light (blue)
647 and dark (beige) cycles. (A) Daily food intake in grams in male and (C) female mice. Average
648 weekly food intake by mass in the light and dark cycle in (B) male mice and in (D) female mice.
649 (E) Daily caloric intake in male and (G) female mice. Average weekly caloric intake in the light

650 and dark cycle in (F) male mice and in (H) female mice. (I) Daily energy expenditure in male
651 and (K) female mice. Average weekly energy expenditure in the light and dark cycle in (J) male
652 mice and in (L) female mice. (M) Daily respiratory exchange ratio in male and (O) female mice.
653 Average weekly respiratory exchange ratio in the light and dark cycle in (N) male mice and in
654 (P) female mice. (Q) Daily water intake in male and (S) female mice. Average weekly water
655 intake in the light and dark cycle in (R) male mice and in (T) female mice. (U) Daily locomotor
656 activity in male and (W) female mice. Average weekly locomotor activity in the light and dark
657 cycle in (V) male mice and in (X) female mice. Data are shown as mean ± SEM for *N*=8 per sex
658 and were statistically analyzed using a repeated measures one-way ANOVA with Tukey
659 multiple comparison tests. P-value definitions: not-significant (ns) >0.05, * <0.05, **<0.01,
660 ***<0.001, **** <0.00001.

661

662 **Supplemental Figure 7. Metabolic phenotyping of mice switched to 45% HFD.** Metabolic
663 parameters in male (black) and female (pink) mice fed a chow diet and switched to 45% HFD
664 for 21 days. (A) ANCOVA of average weekly energy expenditure with body weight as a
665 covariate. (B) Body composition in chow-fed (Pre) and at the end of 21 days of HFD feeding
666 (Post). (C) Daily and average weekly respiratory exchange ratio in male and (D) female mice.
667 (E) Daily and average weekly water intake in male and (F) female mice. (G) Daily and average
668 weekly locomotor activity in male and (H) female mice. Data are shown as mean ± SEM for *N*=8
669 per sex and were statistically analyzed using a repeated measures one-way ANOVA with Tukey

670 multiple comparison tests. P-value definitions: not-significant (ns) >0.05, * <0.05, **<0.01,
671 ***<0.001, **** <0.00001.

672

673 **Supplemental Figure 8. Feeding behaviors in mice switched to 45% HFD separated by light-**
674 **dark cycle.** Feeding behavior analysis in male and female mice switched from chow to 45%
675 HFD on day 0 (dashed lines) in metabolic chambers and divided by light (blue) and dark (beige)
676 cycles. (A) Daily and (B) average weekly meal number in male and (C) daily and (D) average
677 weekly meal number in female mice. (E) Daily and (F) average weekly inter-meal interval in
678 male mice and (G) daily and (H) average weekly inter-meal interval in female mice. (I) Daily
679 and (J) average weekly meal duration in male mice and (K) daily and (L) average weekly meal
680 duration in female mice. (M) Daily and (N) average weekly meal size by mass in male mice and
681 (O) daily and (P) average weekly meal size by mass in female mice. (Q) Daily and (R) average
682 weekly meal size by calorie in male mice and (S) daily and (T) average weekly meal size by
683 calorie in female mice. (U) Daily and (V) average weekly meal rate in grams per minute in male
684 mice and (W) daily and (X) average weekly meal rate in grams per minute in female mice. (Y)
685 Daily and (Z) average weekly meal rate in calories per minute in male mice and (AA) Daily and
686 (AB) average weekly meal rate in calories per minute in female mice. Data are shown as mean ±
687 SEM for *N*=8 per sex and were statistically analyzed using repeated measures one-way ANOVA
688 with Tukey multiple comparison tests. P-value definitions: not-significant (ns) >0.05, * <0.05,
689 **<0.01, ***<0.001, **** <0.00001.

690

691 **Supplemental Figure 9. Effects of sex on 45% HFD-induced changes in metabolic parameters**
692 **and meal patterns.** Average weekly data are shown for male (black symbols) and female (pink
693 symbols) mice as both absolute values and values normalized to chow for each individual
694 mouse across 24-hour cycles. (A) Food intake by mass. (B) Energy intake by calorie. (C) Energy
695 expenditure. (D) Body weight. (E) Meal number. (F) Meal size by mass. (G) Meal size by calorie.
696 (H) Meal duration. (I) Meal rate by mass. (J) Meal rate by calorie. Data are shown as mean ±
697 SEM for *N*=8 per sex and were statistically analyzed using two-way ANOVA with Sidak
698 multiple comparison test. P-value definitions: not-significant (ns) >0.05, * <0.05, **<0.01,
699 ***<0.001, **** <0.00001.

700

701 **Supplemental Figure 10. Shifts in meal patterns across time and light-cycle in mice fed**
702 **obesogenic diets.** Frequency distribution of Type I-IV meals in male and female mice fed chow
703 and then switched to 60% HFD (A-D) or 45% HFD (E-H). (A, E) Type I (<60 mg), (B, F) Type II
704 (<160 mg), (C, G) Type III (<280 mg), (D, H) Type IV (>280 mg) meals. Data are shown as mean ±
705 SEM for *N*=8 per sex and were statistically analyzed using a repeated measures one-way
706 ANOVA with Tukey multiple comparison tests. P-value definitions: not-significant (ns) >0.05, *
707 <0.05, **<0.01, ***<0.001, **** <0.00001.

708

709 **Supplemental Figure 11. Metabolic phenotyping of mice switched to 60% HFD with running**
710 **wheel access.** Metabolic parameters in male mice switched from chow to a 60% HFD at day 0
711 (dashed line) in metabolic chambers with wheels locked or wheels unlocked. (A) ANCOVA of

712 average weekly energy expenditure with body weight as a covariate. (B) Average weekly energy
713 expenditure during the light and dark cycles. (C) Average weekly energy balance. (D) Average
714 weekly body weight and body composition. (E) Daily and average weekly respiratory exchange
715 ratio and (F) average weekly respiratory exchange ratio during the light and dark cycle. (G)
716 Daily and average weekly water intake and (H) average weekly water intake during the light
717 and dark cycle. (I) Daily and average weekly off-wheel activity and (J) average weekly off-
718 wheel activity during the light and dark cycle. (K) Daily and average weekly running wheel
719 activity and (L) average weekly running wheel activity during the light cycle and dark cycle in
720 mice with access to unlocked running wheels. Data are shown as mean ± SEM for *N*=8 per
721 group and were statistically analyzed using a two-way ANOVA with Sidaks multiple
722 comparison tests. P-value definitions: not-significant (ns) >0.05, * <0.05, **<0.01, ***<0.001, ****
723 <0.00001.

724

725 **Supplemental Figure 12. Effects of running wheel access on feeding behaviors and meal**
726 **patterns.** Feeding behavior and meal type analysis by light-dark cycle in male mice switched
727 from chow to a 60% HFD with access to locked or unlocked running wheels. Average weekly
728 (A) food intake by mass, (B) energy intake by calorie, (C) meal numbers, (D) inter-meal interval,
729 (E) meal duration, (F) meal size by mass (G) meal size by calorie, (H) meal rates by grams per
730 minute, and (I) meal rates by calories per minute. Mice with locked wheels are shown in light
731 gray (light cycle) and dark gray (dark cycle) bars with data points depicted by circles. Mice with
732 unlocked wheels are shown in orange (light cycle) and blue (dark cycle) with data points

depicted by squares. Frequency of meal types [Type I (<60 mg), Type II (<160 mg), Type III (<280 mg), Type IV (>280] across time on diet in mice with (J) wheels locked and (K) wheels unlocked. (L) Frequency of meal types across time on diet in mice with wheels locked vs. wheels unlocked. Data are shown as mean ± SEM for *N*=8 per group and were statistically analyzed using a two-way ANOVA with Sidaks multiple comparison tests. P-value definitions: not-significant (ns) >0.05, * <0.05, **<0.01, ***<0.001, **** <0.00001.

Figure 1. Food intake and energy balance in mice fed a 60% high-fat diet

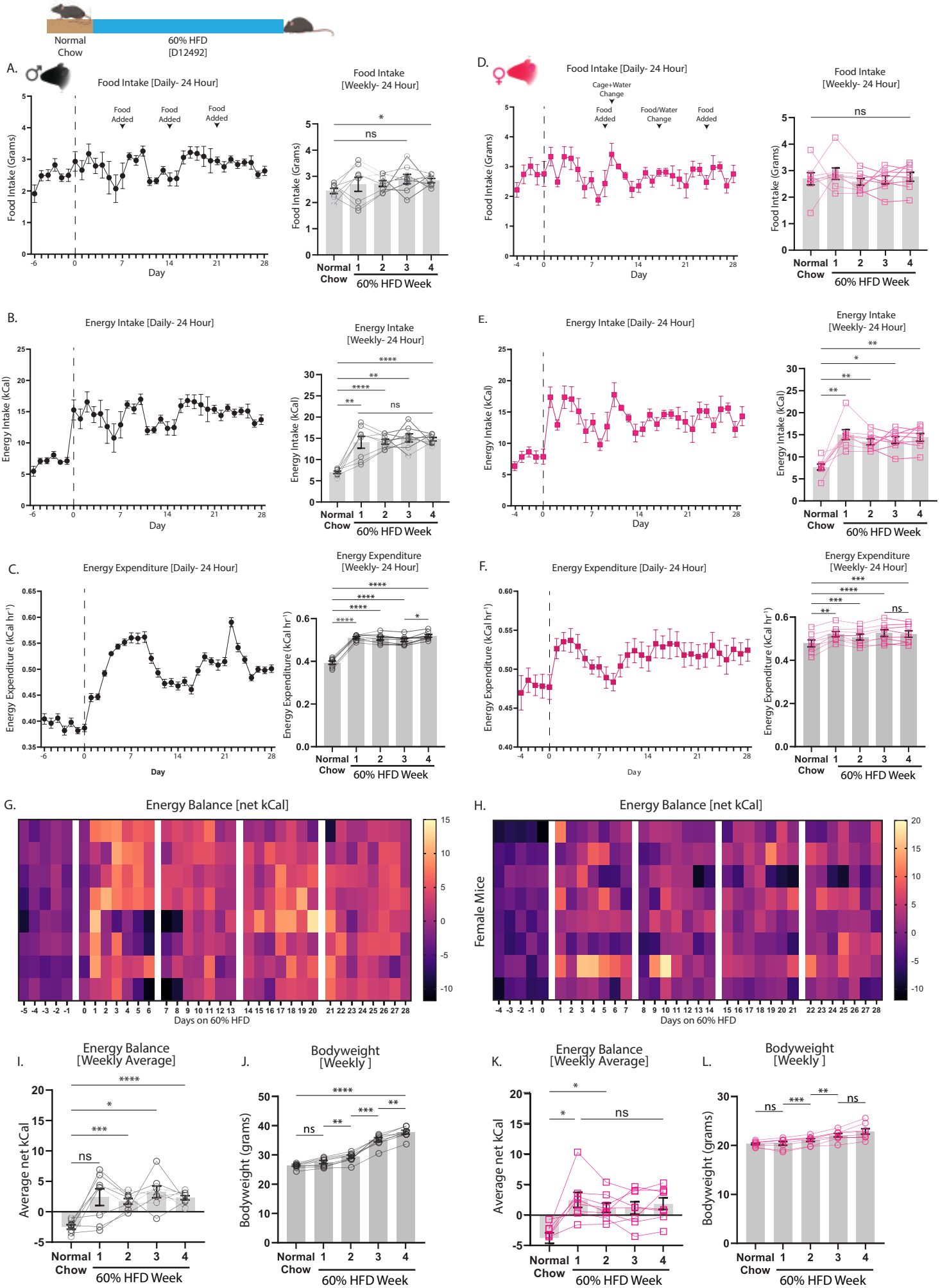

Figure 2. Feeding behaviors in mice switched to 60% high-fat diet

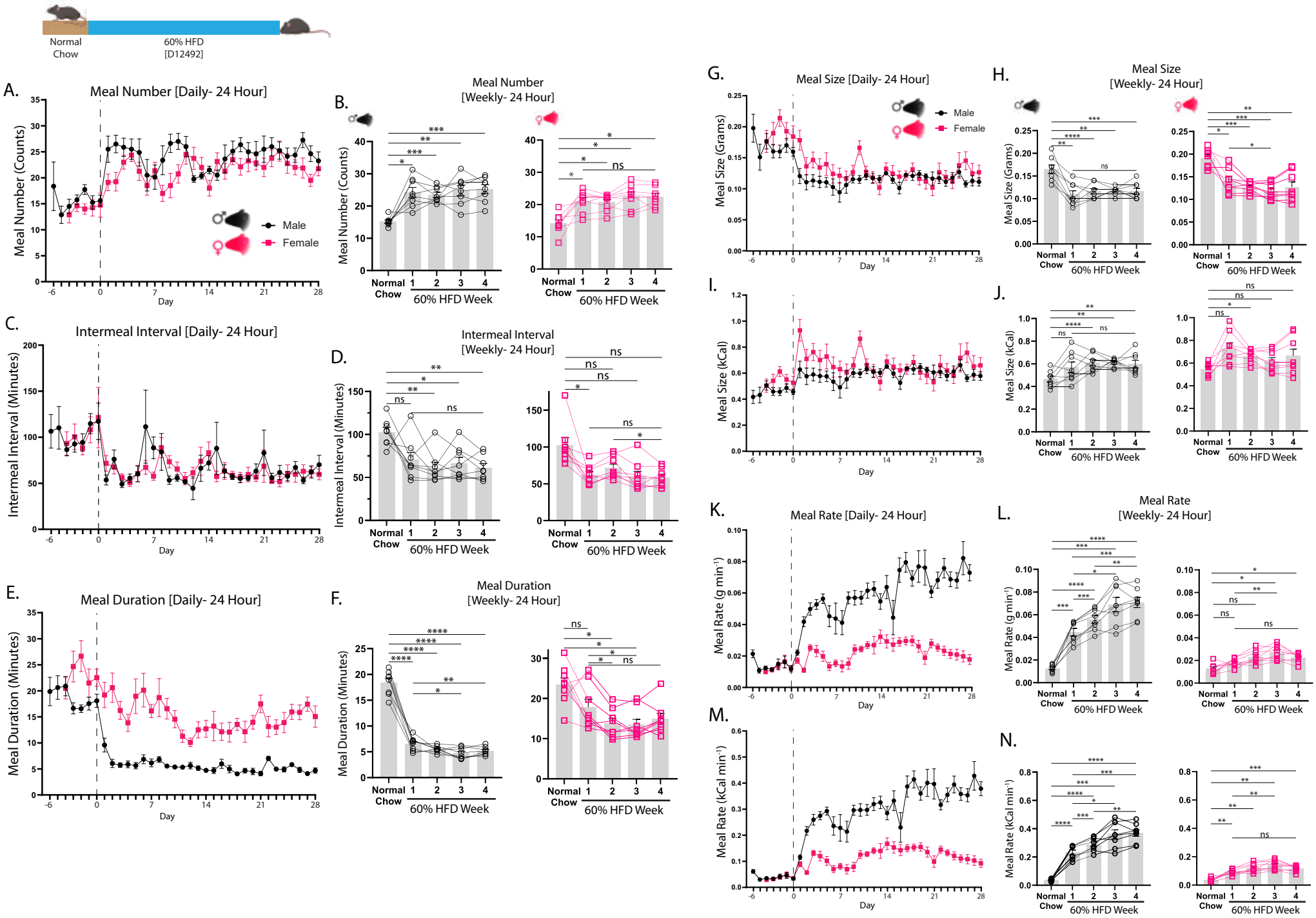

Figure 3. Food intake and energy balance in mice swithced to a 45% high-fat diet

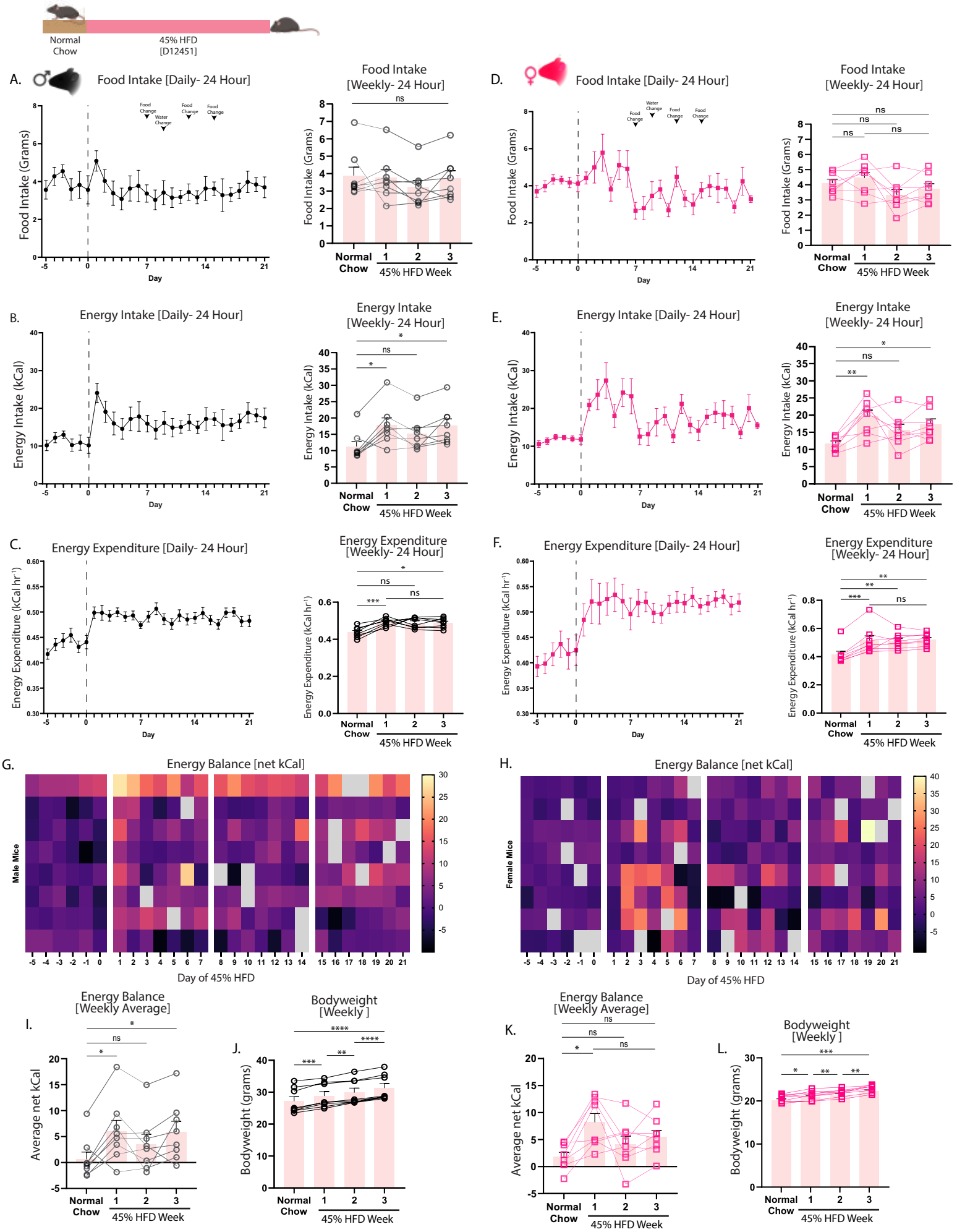

Figure 4. Daily and weekly feeding behaviors in mice fed a 45% high-fat diet

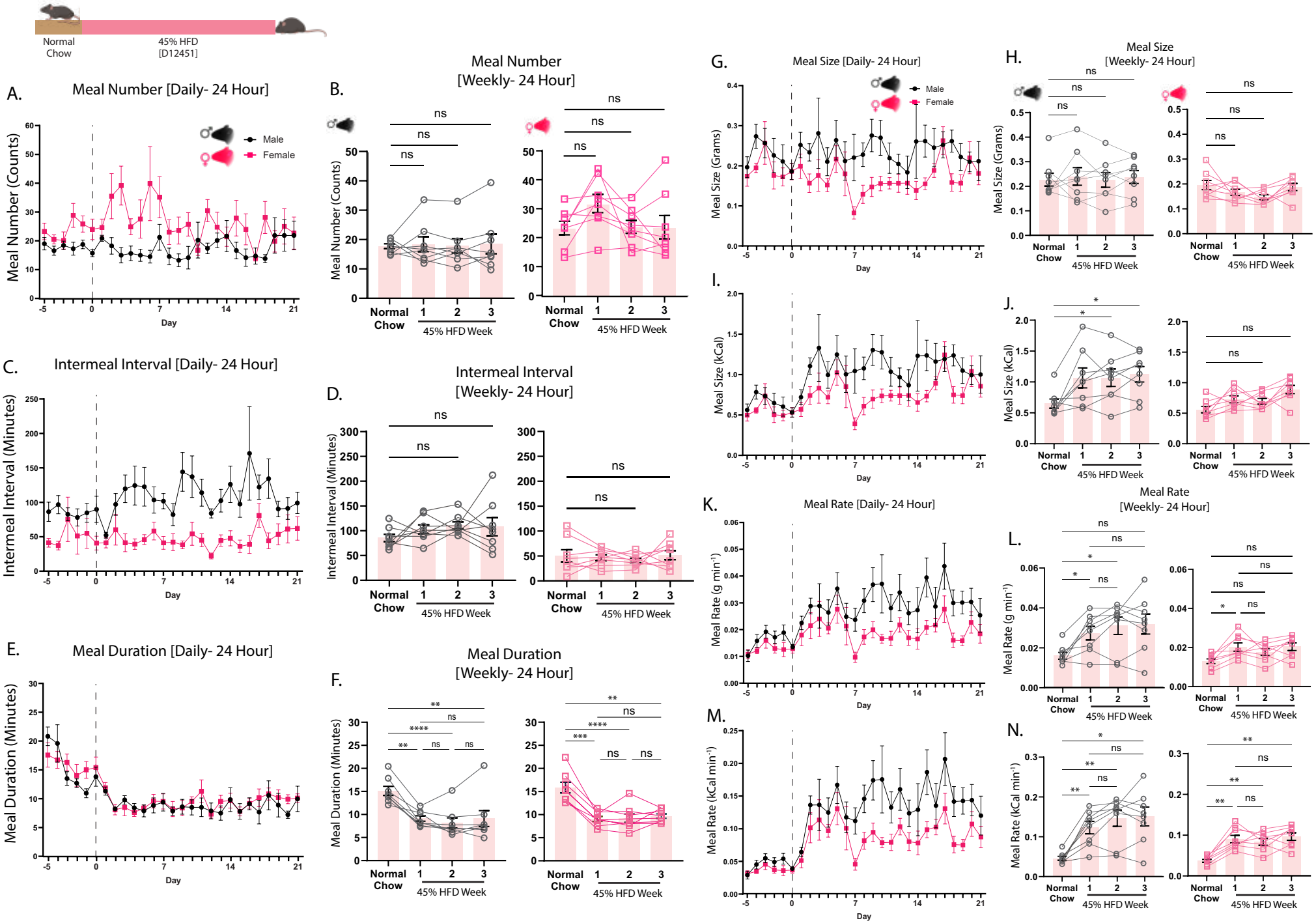

Figure 5. Meal patterns of male and female mice fed obesogenic diets

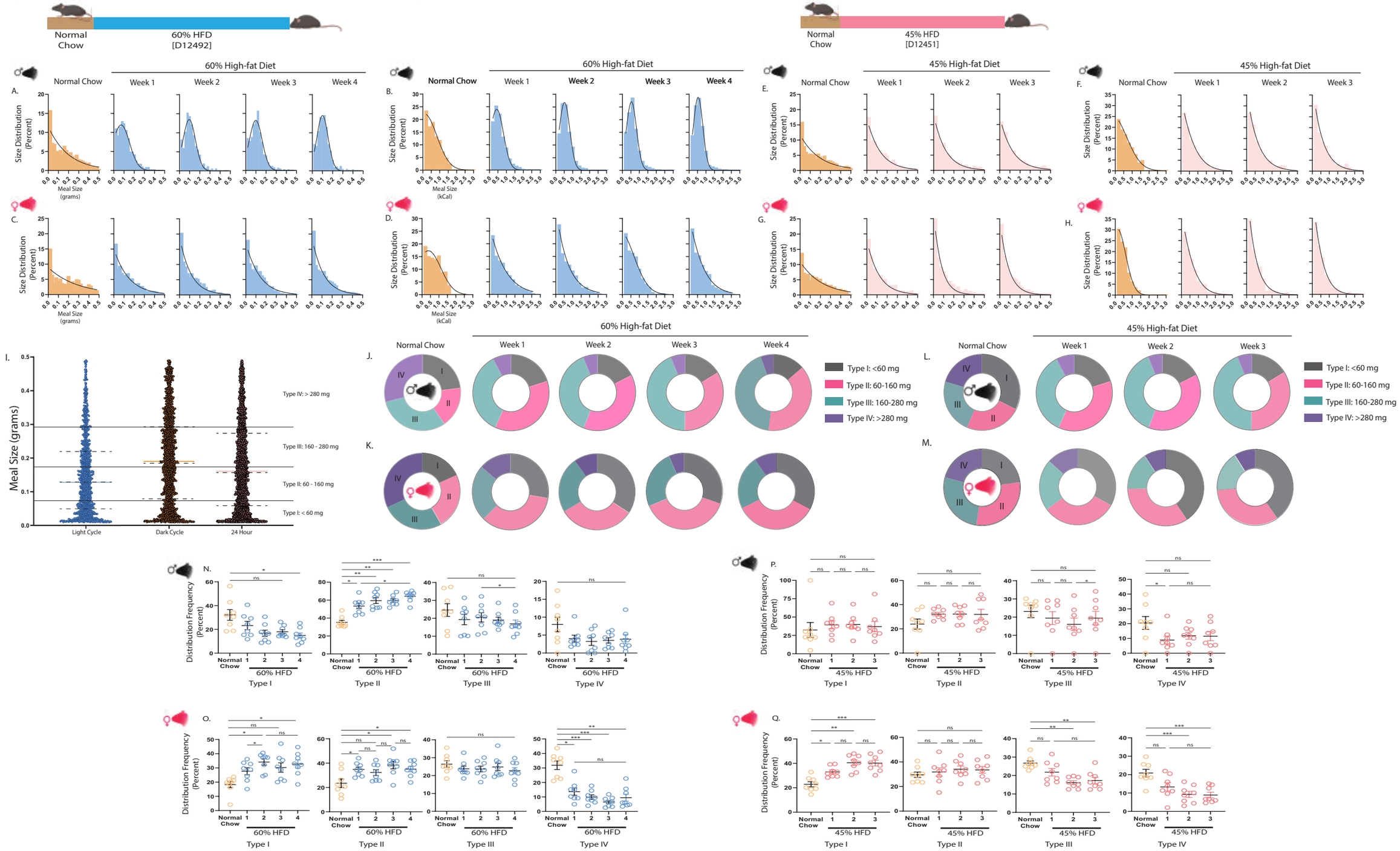

Figure 6. Effects of running wheel access on feeding behavior and energy expenditure in male mice switched to a 60% high-fat diet

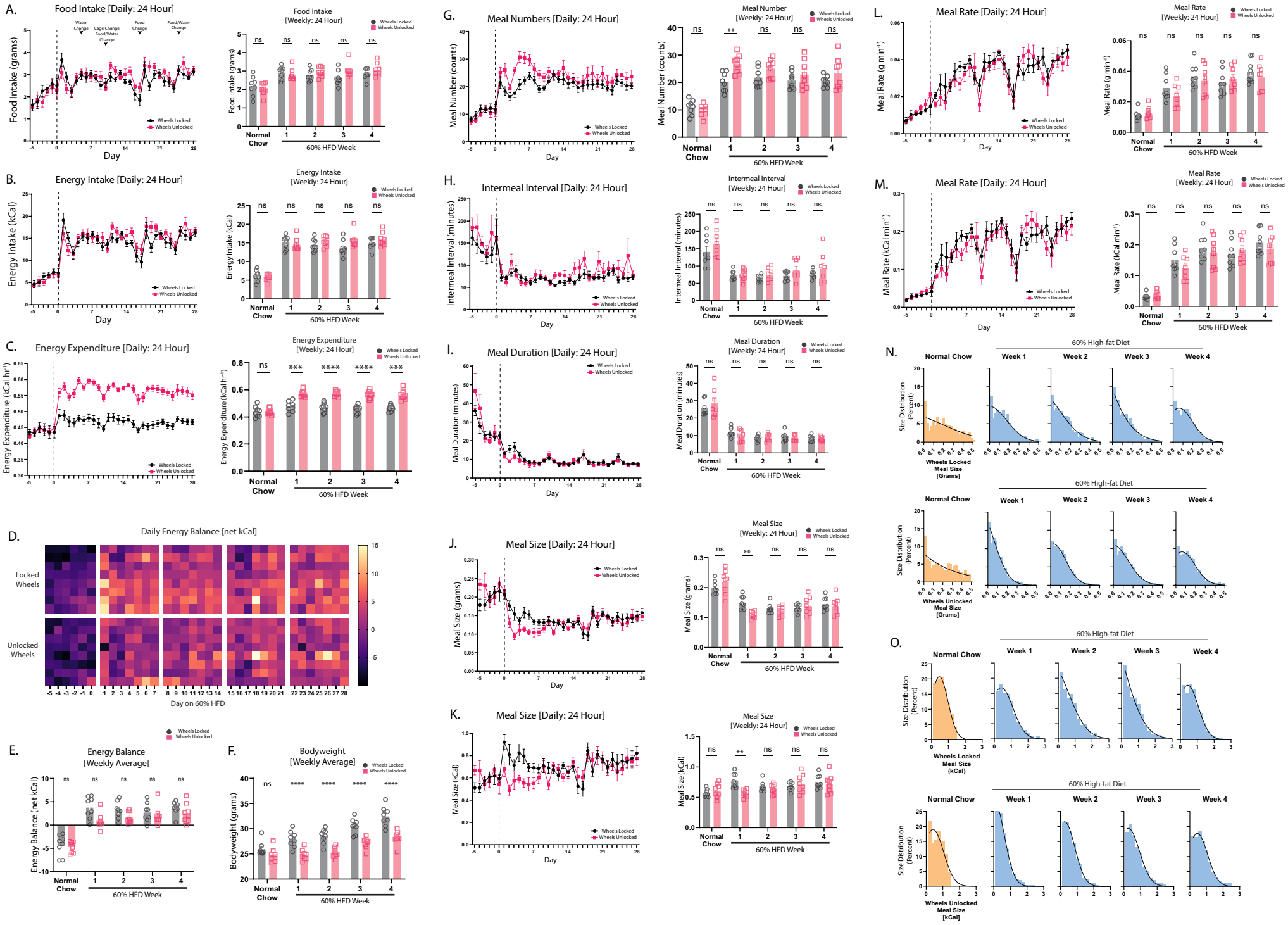

Supplemental Figure 1. Metabolic phenotyping of mice switched to a 60% high-fat diet [light-dark cycle]

Supplemental Figure 2. Metabolic phenotyping of mice switched to a 60% high-fat diet

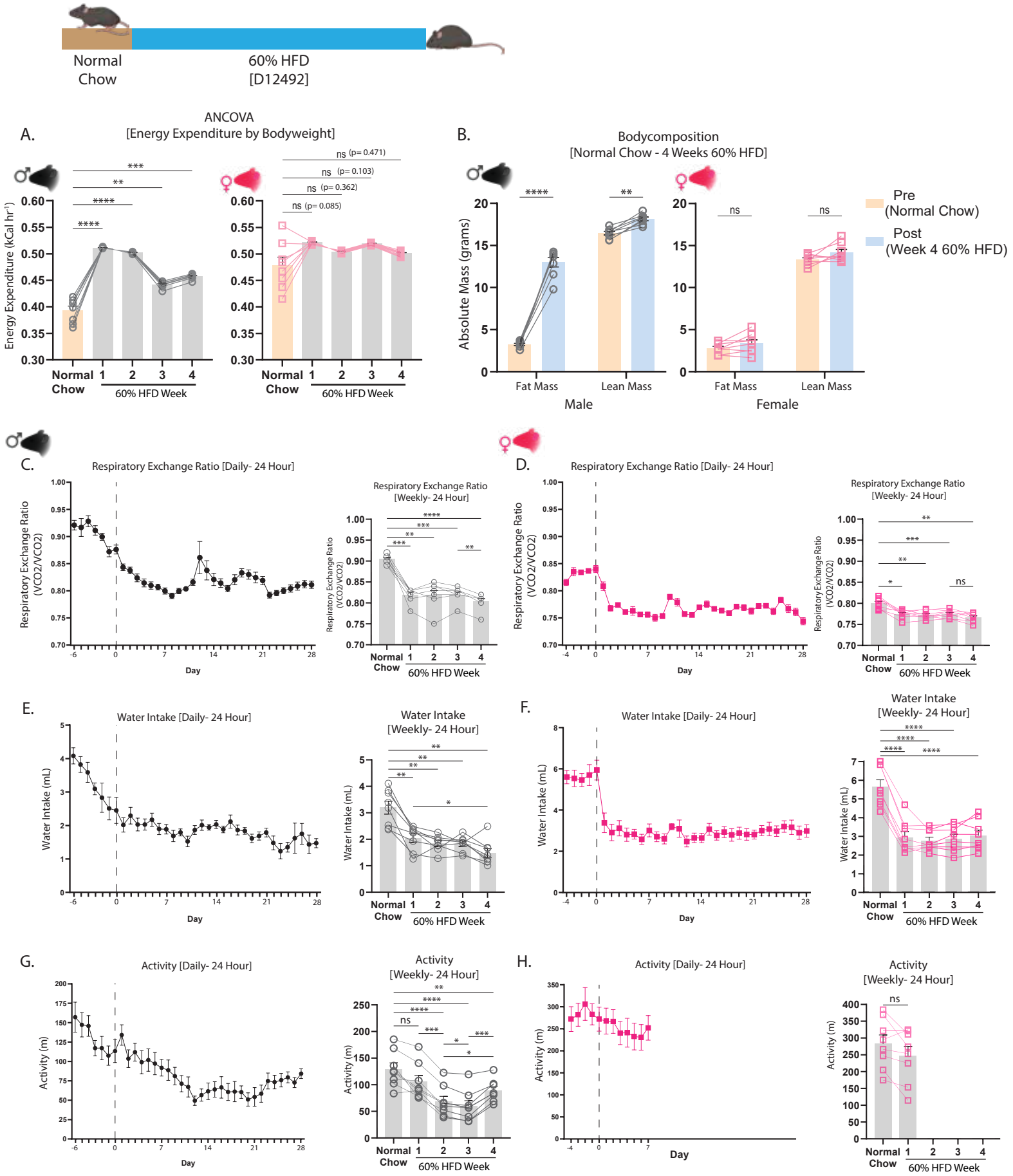

Supplemental Figure 3. Feeding behavior of mice switched to a 60% high-fat diet [light-dark cycle]

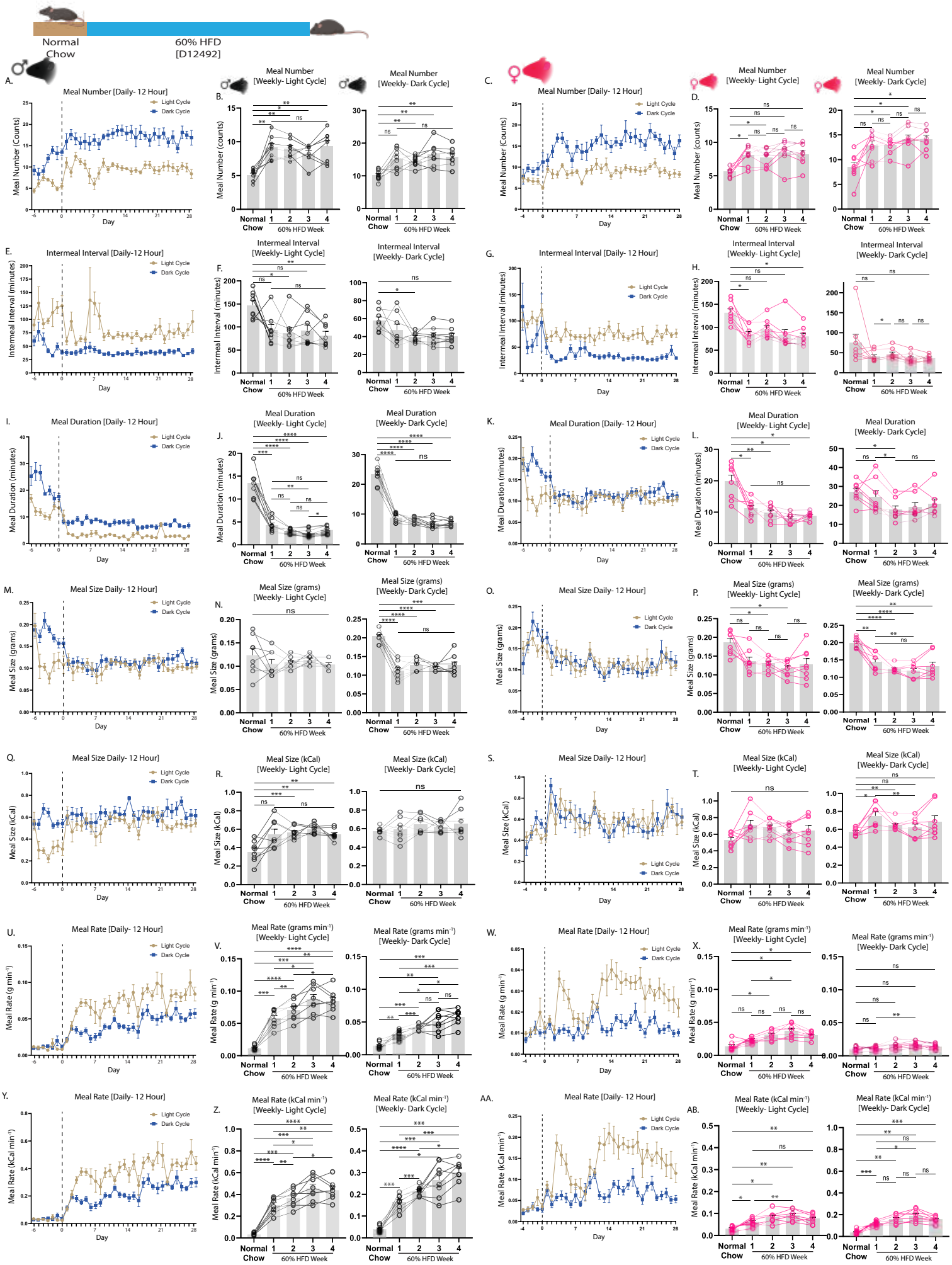

Supplemental Figure 4. Food Intake, Energy Expenditure, and Feeding Behaviors in mice retained on Normal Chow or administered a 60% High-fat Diet

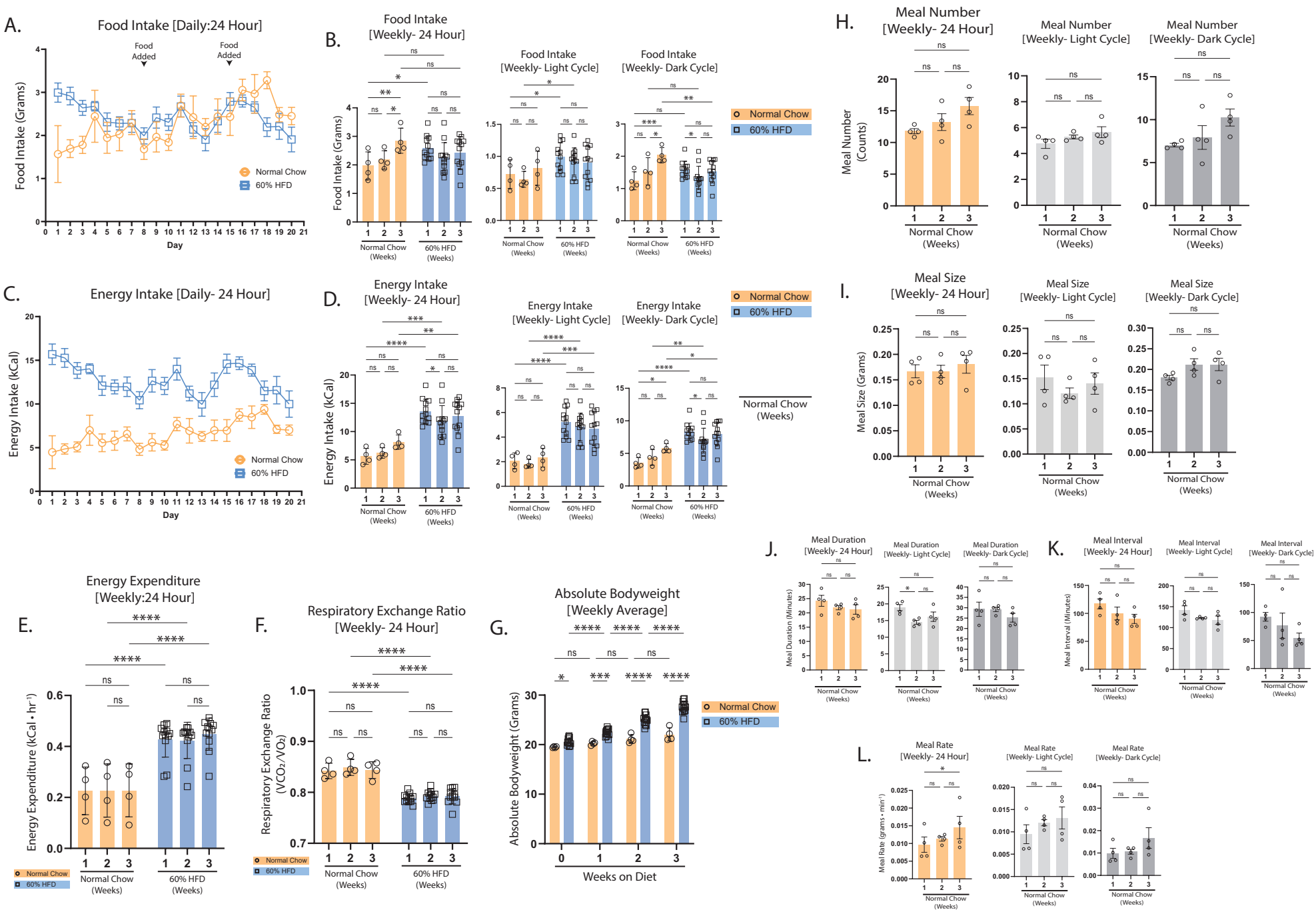

Supplemental Figure 5. Effects of sex on 60% HFD induced changes in energy expenditure, food intake, and feeding behaviors

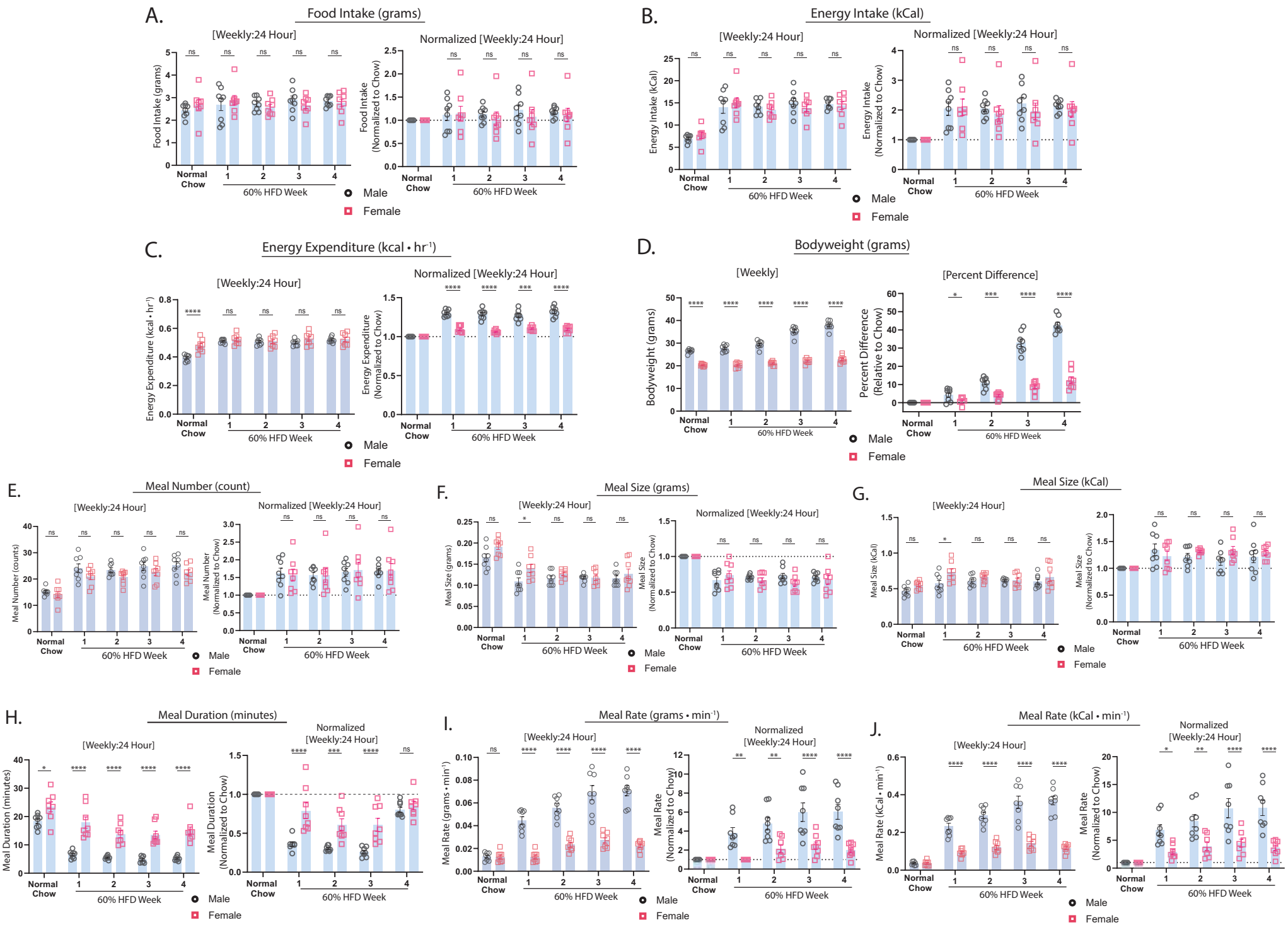

Supplemental Figure 6. Metabolic Phenotyping of of mice switched to a 45% high-fat diet [light-dark cycle]

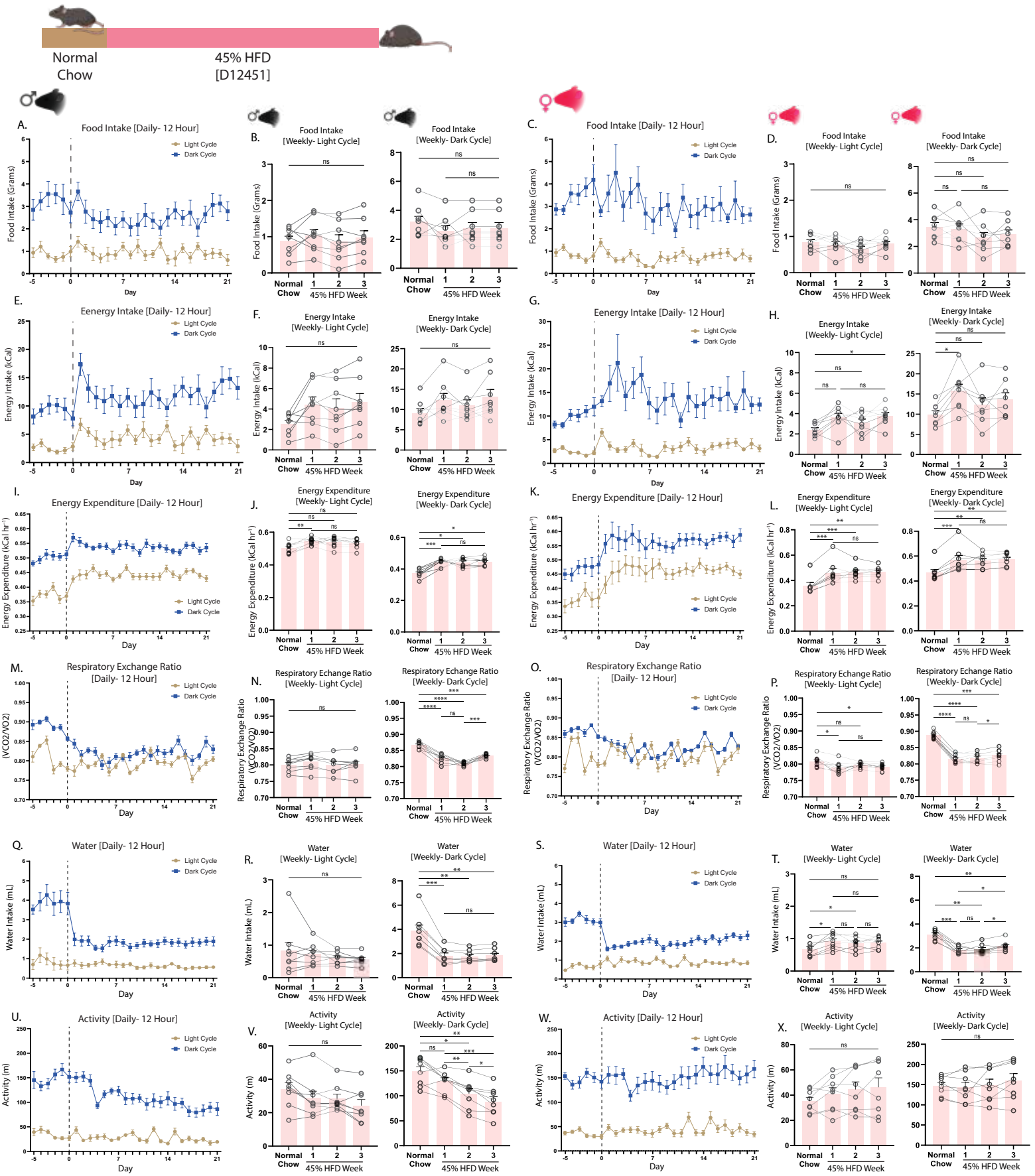

Supplemental Figure 7. Metabolic phenotyping of mice switched to a 45% high-fat diet

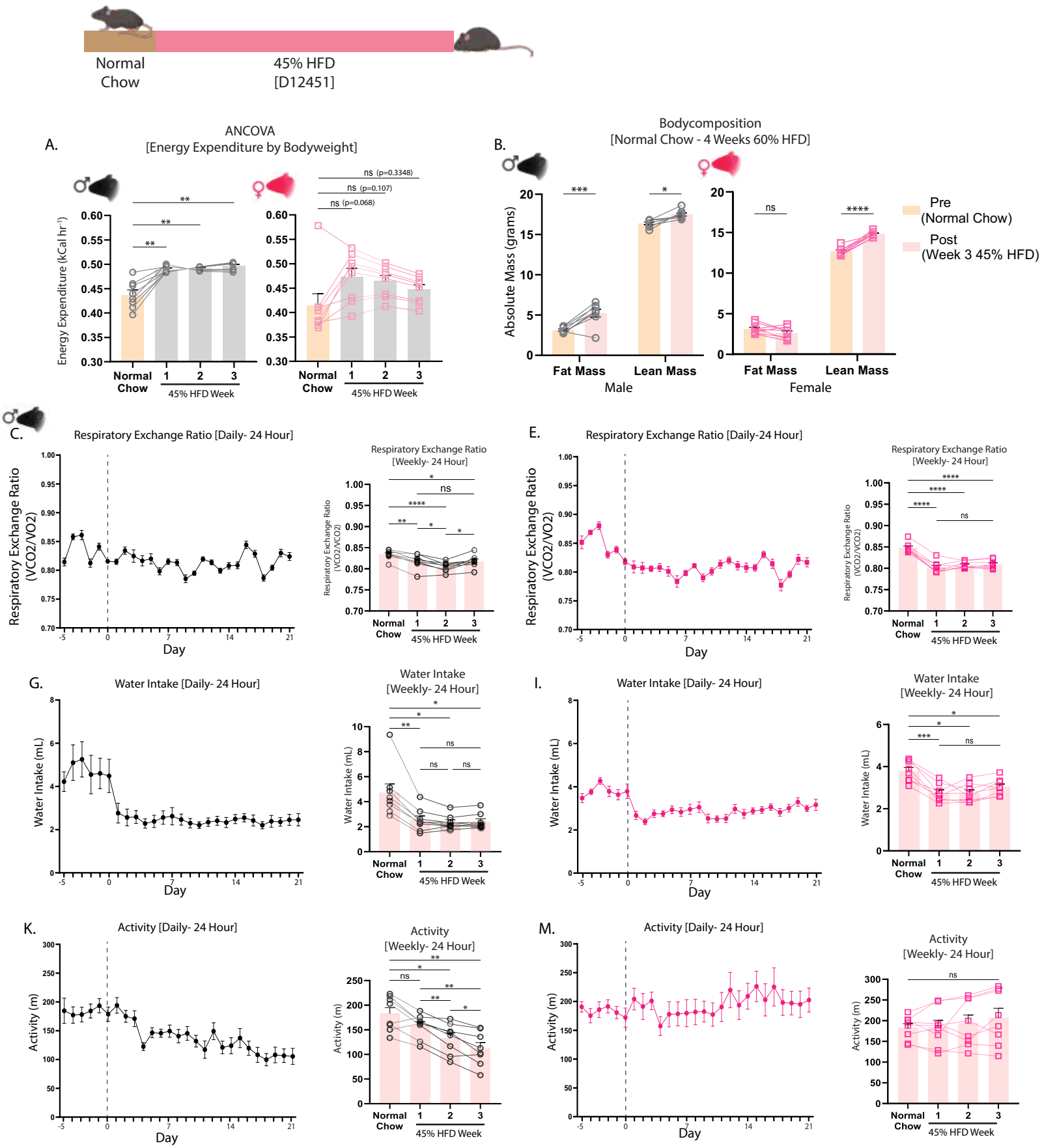

Supplemental Figure 8. Feeding behavior of mice switched to a 45% high-fat diet [light-dark cycle]

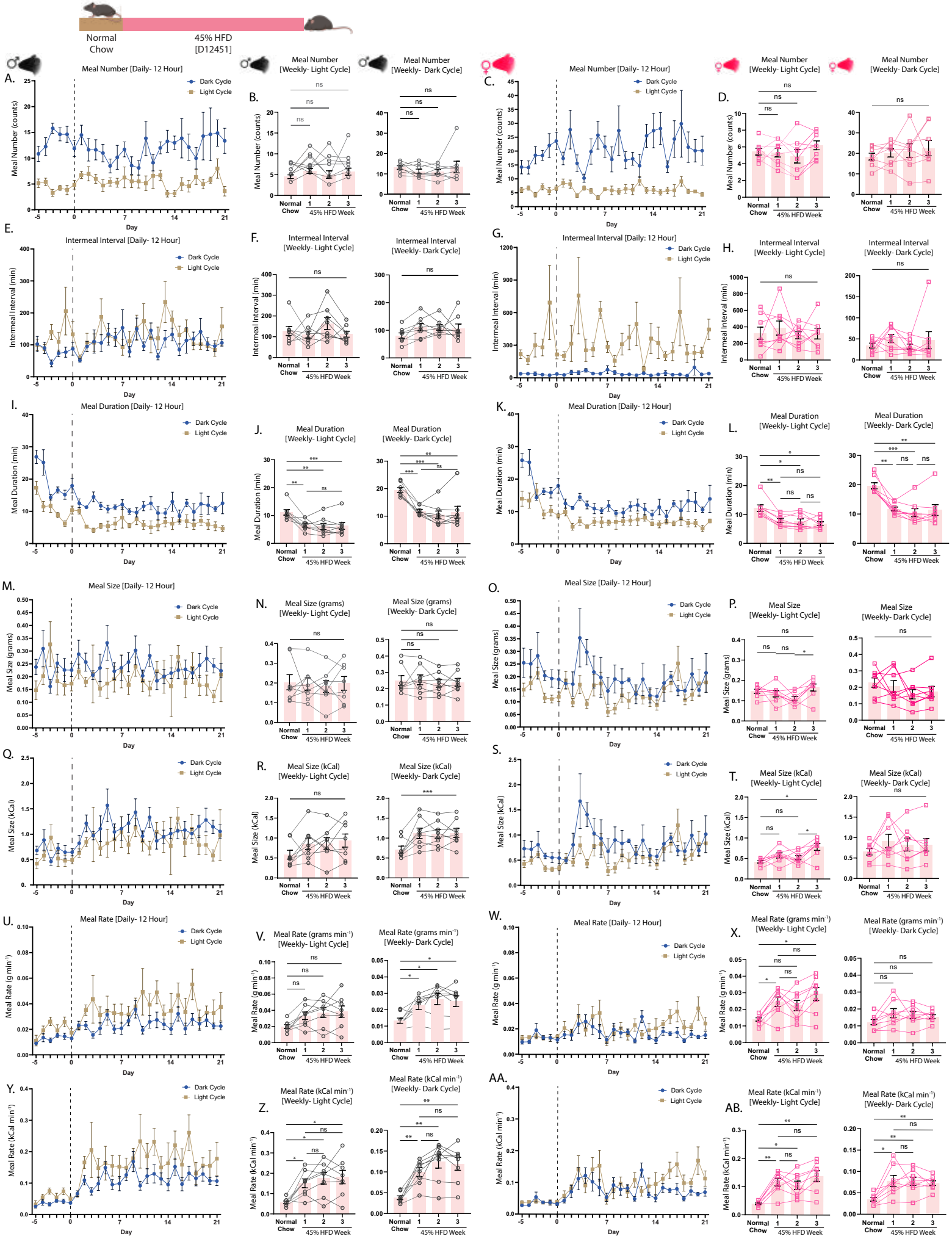

Supplemental Figure 9. Effects of sex on 45% HFD induced changes in energy expenditure, food intake, and feeding behaviors

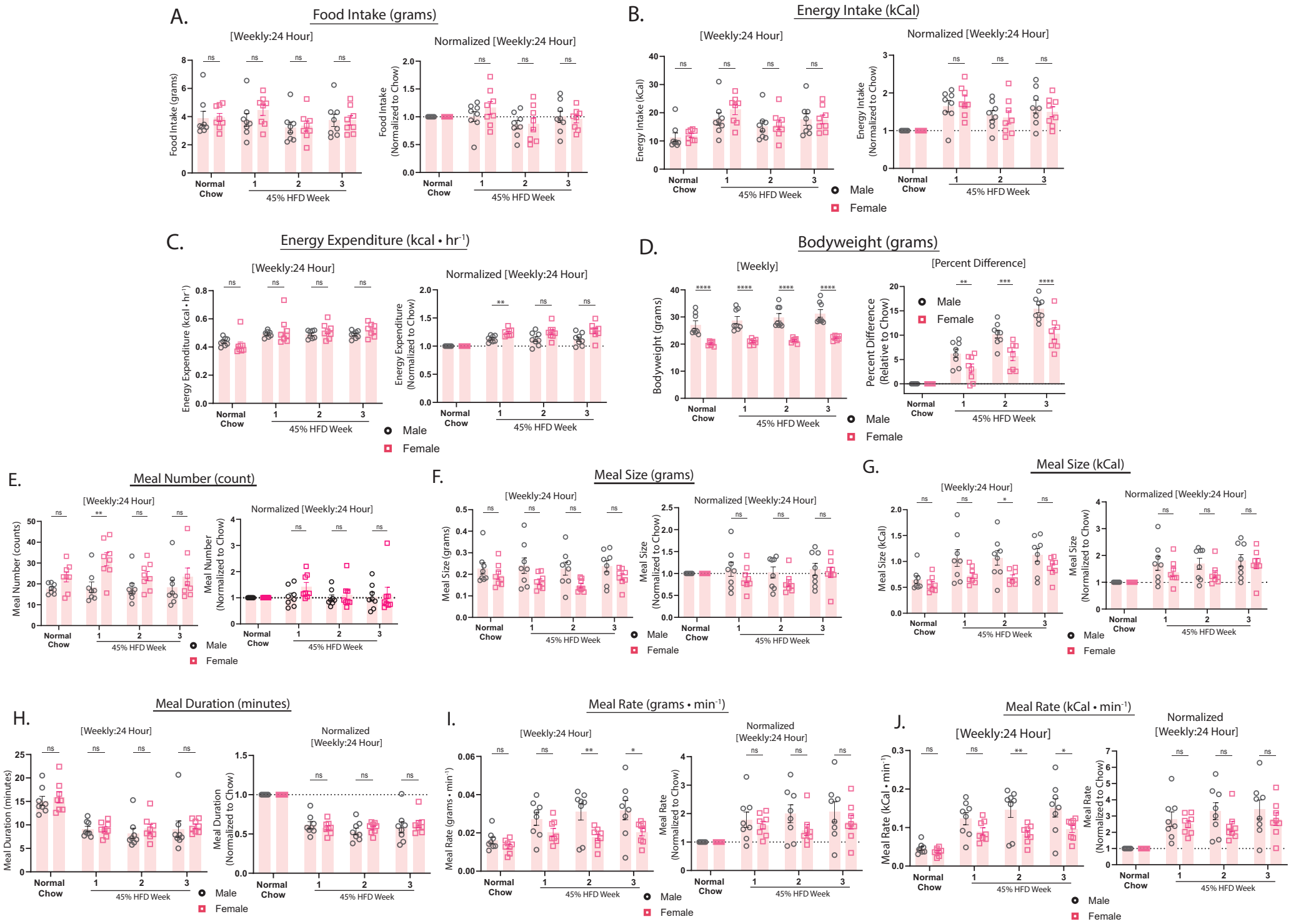

Supplemental Figure 10. Shifts in meal patterns across time and light-cycle in mice fed obesogenic diets

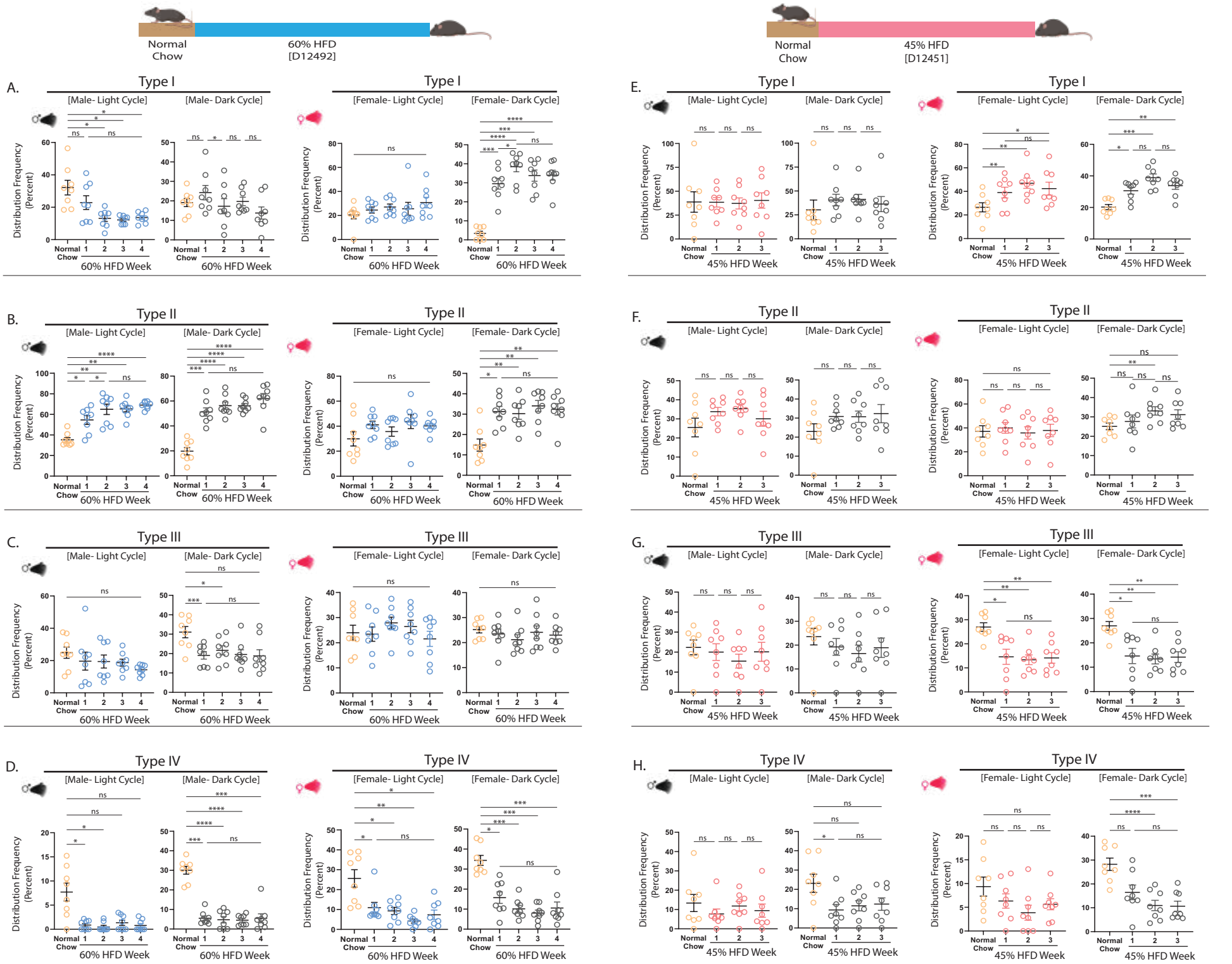

Supplemental Figure 11. Metabolic phenotyping of mice switched to a 60% HFD with running wheel access

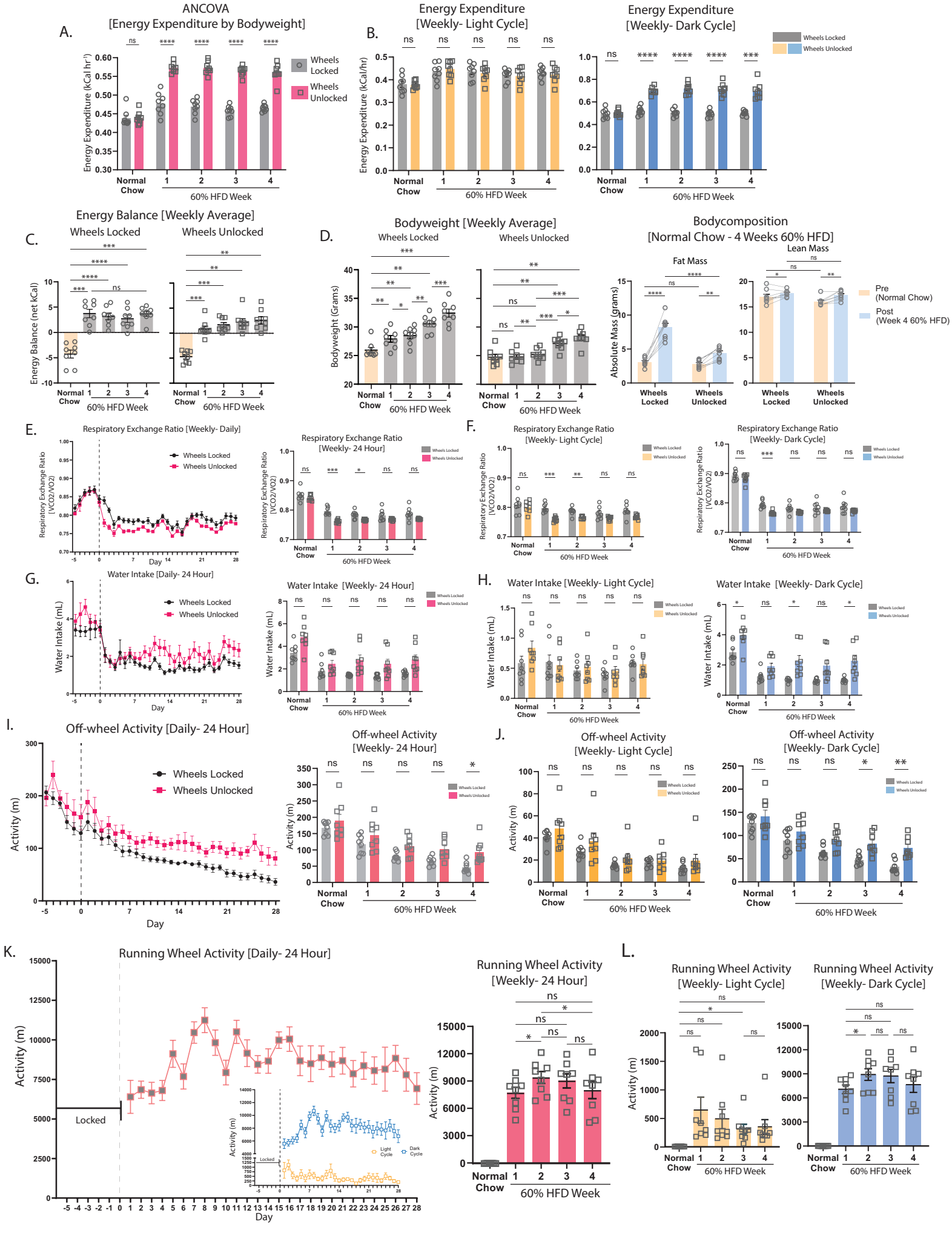
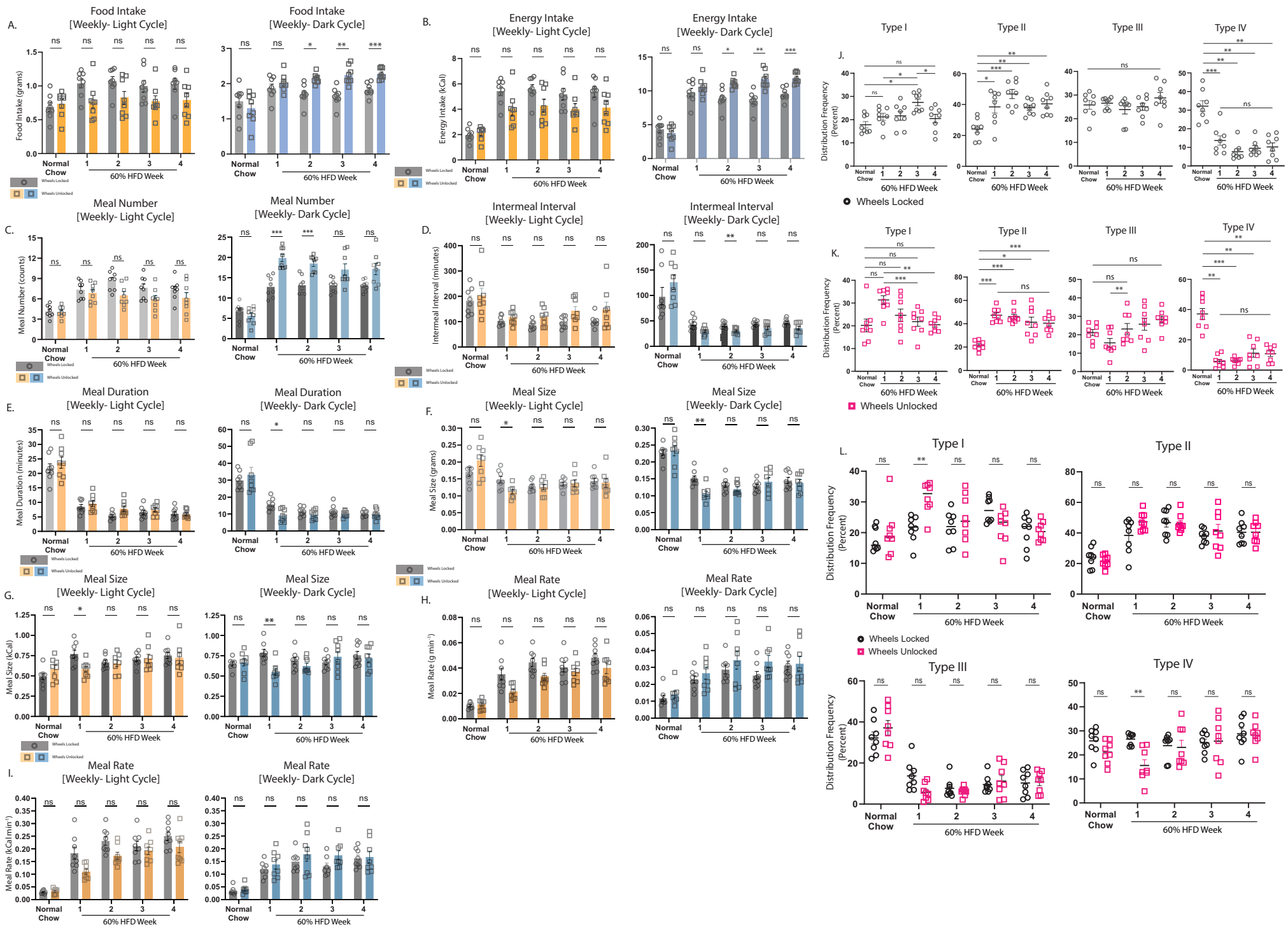
Supplemental Figure 12. Effects of running wheel access on feeding behavior and meal patterns